

Working Paper 159 | May 2024

Modeling Direct and Indirect Climate-related Physical Risks

Document for the exclusive attention of professional clients, investment services providers and any other professional of the financial industry

Trust
must be earned

Amundi
ASSET MANAGEMENT

Modeling Direct and Indirect Climate-related Physical Risks

Abstract

Faustine DE MAXIMY

Centrale Supélec

faustine.de-maximy@student-cs.fr

Vincent POUDEROUX

Amundi Technology

vincent.pouderoux@amundi.com

Theo LE GUENEDAL

Amundi Technology

theo.leguenedal-ext@amundi.com

This paper addresses the methodological challenges in quantifying physical risks associated with climate change, proposing a novel top-down stochastic approach focused on modeling financial losses from extreme events. Unlike existing studies limited to specific events, our approach utilizes predefined climate sensitivity parameters, enabling a broader application across various extreme events using the example of tropical cyclones. We have also conducted an extended review of the literature on the modeling of indirect shocks to cover the full scope of the damage modeling from cost-push Leontief price model to Adaptive Regional Input-Output approaches (ARIO, Hallegatte, 2013). Building on Desnos et al. (2023)'s adaptation of the value-at-risk concept for transition risk analysis, we extend the framework to incorporate direct physical shock impacts with co-occurrence, cascading effects through input-output mechanisms (indirect damages to the economy), and temporal considerations (forward projection, capacity for a sector to rebuild itself). By bridging the gap between these two approaches, we provide a comprehensive assessment of climate risks, considering uncertainties associated with transition scenarios and offering insights into the amplification of impacts through time and across global economies.

Keywords: Climate change, physical risks, Monte Carlo simulation, damage modeling, indirect risk, adaptive input-output.

JEL classification: C6, G12, H63, Q54

Acknowledgement

The authors are very grateful to Thierry Roncalli, Peter Tankov, Raphael Semet, Jiali Xu and Samuel Juhel for helpful comments.

About the authors



Faustine DE MAXIMY

Faustine de Maximy joined Amundi Technology's Innovation Lab as a Gap Year intern from July 2023 to January 2024 to work on the Modeling Direct and Indirect Climate-related Physical Risks project with Théo Le Guenedal and Vincent Pouderoux. Prior to this, she was studying at CentraleSupélec, a prestigious engineering school, where she pursued several programs in Statistics & Probability, Optimization, PDE and integration, ML & Computer Science. Subsequently, she worked as a Data Scientist intern on quantitative models at the AdTech company Criteo to complete her Gap Year. Following this, she will finish her Master of Engineering at CentraleSupélec, which she began in 2021. During the last year of her studies, she plans to specialize in Mathematics & Data Science and also complete a Mathematics-focused Master's degree concurrently with her studies at CentraleSupélec.



Vincent POUDEIROUX

Vincent Pouderoux has joined Amundi Technology's Innovation Lab in January 2022 as a Quantitative Project Manager. He has been working jointly with Theo Le Guenedal on Prospective Research topics since January 2024. Prior to this, we has 15 years of experience in Finance and Asset Management, and has headed for 18 months a project to integrate extra financial criteria in the financial decision using artificial intelligence, with direct report to Societe Generale's Group Executive Committee. He has worked for 5 years in a multi-rewarded (European level) systematic CTA Hedge fund. He also has 2 years of experience in the 10+ billion AUM Fixed Income, and 3 years in the volatility departments of Lyxor Asset Management. He has participated to the United Nations initiative for Positive Impact Finance. He has worked on quantitative strategies design and implementation, optimization, liquidity stress testing, derivative's pricing, algorithmic trading, systems design and implementation and is contributor and author of various research papers and financial studies on asset management and climate. He holds a master's Degree in Applied Mathematics from Paris IX Dauphine and Pantheon Sorbonne universities.



Theo LE GUENEDAL

Dr. Théo Le Guenedal currently leads Prospective and Climate Research at Amundi Technology's Innovation Lab. Recently, he has been focusing on the integration of advanced climate metrics, stress tests, and analytics in investment tools at Amundi Technology's Innovation Lab. Prior to this, he worked in the Quantitative Research team at Amundi Institute (AM), starting with a project on the performance of ESG investing in the equity market in December 2018. Since then, he has been involved in an extensive research project on the incorporation of ESG factors and climate risks into asset allocation strategies. He completed his Ph.D. thesis entitled "Financial Modeling of Climate-related Risks" in Applied Mathematics at the Institut Polytechnique in December 2023. This research covers both transition and physical risks. On this occasion, Théo co-authored a paper entitled "Credit Risk Sensitivity to Carbon Price." This work was recognized with the GRASFI Best Paper Prize for Research on Climate Finance, a distinguished honor sponsored by Imperial College London, in 2020. On the subject of physical risks, Théo also made significant contributions to the academic domain of physical risk assessment by creating the Tropical Cyclone Generation Algorithm.

Table of Contents

1	Introduction	8
2	Direct damage modeling	12
2.1	Bottom-up approach: Case of tropical cyclones	12
2.1.1	Local damage functions	15
2.1.2	Asset exposure	16
2.2	Top-down approach: stochastic shock matrix	20
2.2.1	Modeling occurrences of extreme events	20
2.2.2	Downscaling of the shocks	20
2.2.3	Top-down damage function	23
3	Modeling indirect effects of physical shocks	25
3.1	Classical input-output diffusion through sector requirements	25
3.2	Optimal production after extreme events	32
3.3	Adaptive regional input-output (ARIO) model	38
3.3.1	Seminal adaptive framework (Hallegatte, 2008)	38
3.3.2	Implementing the ARIO approach (BoARIO, Hallegatte, 2013)	43
3.4	Comparison of diffusion approaches	50
4	Physical Value-at-Risk and Empirical Applications	51
4.1	Monte Carlo algorithm for direct damages	51
4.2	Results and Operational Implication	52
5	Conclusion	60
A	Notation	65
B	Complementary materials	66

1 Introduction

Following Bank of England’s governor pivotal address Carney (2015), the financial community has begun to more seriously consider climate-related risks. Regulatory bodies and central banking officials have specifically urged financial institutions to implement stress-testing systems to quantify their exposure to both transition and physical risks (ESMA, 2022). Direct costs of extreme events have a significant impact on economies worldwide, often reaching magnitudes of hundreds of billions of dollars. This paper focuses on the physical risk dimension using the example of tropical cyclones, its amplification coefficient through the supply-chain, adverse effect of supply-chain disruption and post-crisis recovery.

As of 2023, only one in ten companies provides incentives for the management of climate change issues, according to CDP’s Messenger *et al.* (2023), even though 83% of companies are recognizing physical risks as a financial risk for their business. If the current trend continues, the number of disasters could rise to 560 per year by 2030, up 40% as compared to 2015. Up to \$340 billion per year of adaptation finance is needed by 2030 to pay for investments in technology and in transforming agriculture and water systems.

Physical risks are far more difficult to quantify than transition risks as their evaluation requires multidisciplinary methodologies: climate modeling, physical asset geolocation, financial loss estimation, etc. (Le Guenedal, 2022). For example, Le Guenedal *et al.* (2022) measured the impact of cyclone-related damage in the future representative concentration pathways in a Monte-Carlo fashion, and offer an integrated approach to channel the impact to sovereign 10Y treasury bonds spreads - using Hilscher and Nosbusch (2010) approach. This study is limited to direct costs and complex to generalize to other events (floods, droughts, wildfire, etc.) because it requires physical modeling and interdisciplinary approach. Thus, we propose a novel top-down stochastic approach to model the damages caused by extreme events based on predefined climate sensitivity parameters which allow us to focus on the modeling of financial losses, introducing co-occurrence of extreme events.

In the context of transition risk analysis, Desnos *et al.* (2023) introduced a method to adapt the value-at-risk concept to the assessment of climate risks. The probability of extreme losses in a climate value at risk fashion is not calibrated on historical losses but on a wide range of possible transition hypothesis. In particular, this model includes cascading effect occurring through an input-output framework. It also accounts for various additional uncertainties associated with transition scenarios (pass-through, regulatory pressure), allowing practitioners to better understand the level of uncertainty associated with transition scenarios. In this paper, we bridge the gap between the two approaches, allowing direct physical shock impacts to cascade and be amplified through input-output effect within the countries and worldwide (Adenot *et al.*, 2022; Desnos *et al.*, 2023) and through time with rebuilding modeling (Hallegatte, 2013). This paper thus extends Desnos *et al.* (2023) structural climate Value-At-Risk to the physical risks from climate change.

In this paper, we advance the scholarly understanding of physical risk modeling by addressing both direct and indirect dimensions comprehensively. Initially, we undertake a thorough review of existing methodologies for the direct and indirect modeling of physical risks, delineating the procedural steps necessary for the calibration of a bottom-up approach. This approach demands asset-level, geolocated data, and due to its extensive data require-

ments, we defer the empirical application of our model to future research. Concurrently, we explore a top-down method that simplifies computational demands and facilitates the incorporation of the co-occurrence of extreme events through appropriate calibration at both the sectoral and national levels.

Further, we employ a Monte Carlo methodology to model the distribution of direct and indirect economic damages, thereby generating parametric estimates of physical Value-at-Risk (VaR). While our examples are illustrative, we assert that with proper calibration, this model can offer robust operational insights, enhancing the measurement and management of physical risks within portfolios. Additionally, our paper integrates adaptive input-output (IO) approaches to better capture the temporal economic responses following disasters. This integration not only deepens the theoretical framework but also holds practical implications for investment strategies post-disaster. Through these contributions, our study not only enriches the academic discourse on physical risk but also provides a foundational tool for future empirical and theoretical exploration.

The literature on changes in the severity and frequency of acute extreme events and chronic risks is extensive. There is a more or less explicit increase in the intensity of extreme events due to global warming, and these changes need to be measured using climate data produced by the Atmosphere-Ocean Climate General Circulation Models (AOGCMs) of the Coupled Model Intercomparison Project (CMIP), currently in its sixth phase. The IPCC aggregate several studies based on these climate projections, and alert on a series of facts.

For example, using the CGMs of CMIP5, Tabari (2020) reports that approximately 72% of the global land is likely to go through aridification in the future, with substantial changes in MENA, south Europe, south Africa and Australia, leading a shift in climate regime. Globally, arid and semi-arid regions would expand by 10.3% and 9.9% respectively, while humid and semi-humid regions would decrease by 2.3% and 4.9% respectively. It makes the area coverage of humid, semi-humid, semi-arid and arid climates at the end of the 21st century equal to 55%, 20%, 11% and 14% of the total terrestrial land area respectively.

They also found flood intensity increases with global warming at the rates of 5.07%/K for humid, 3.63%/K for semi-humid and 3.12%/K for semi-arid climate regions. Examination of 12 General Circulation Models (GCMs) - in the present and five future CMIP6 SSP forcing scenarios - reveals a global trend where the frequency, duration, and severity of Meteorological Flash Droughts (MFDs) are anticipated to escalate by approximately 20–50%, 20–58%, and 26–62% respectively. Notably, these increases are most probable during the summer months (Sreeparvathy & Srinivas, 2022). For wildfires, some advanced models have also been developed such as BURN-P3 (Parisien *et al.*, 2005).

All together, the use of these models with properly unbiased climate data allows modelers to anticipate changes in exposure to extreme events sensitive to climate change. Based on the suggested variations of droughts, floods from the mentioned literature, and cyclones damages (Le Guenedal *et al.*, 2022), we can propose a new mathematical approach to describe the evolution of return periods of each events depending on its total direct costs.

The indirect effects of tropical cyclones and disaster have been measured in the literature. For example, in the financial sphere, Mandel *et al.* (2021) measured the cascading effect of flood risk within the financial system with a network propagation approach. Fereshtehne-

jad *et al.* (2021) propose a probabilistic risk assessment of coupled natural-physical-social systems exposed to coastal storm. Kunze (2021) shows that the losses induced by tropical cyclones are local and found limited lagged impact of tropical cyclones worldwide using input-output in a panel analysis for a maximum of 205 countries over the 1970–2015 period.

However, Lenzen *et al.* (2019) demonstrates important economic spillovers induced by tropical cyclones focusing on Debbie in Australia in 2017. Their Australian region-based input-output analysis shows that regions not physically impacted by the cyclone were affected economically (job losses, reduced activity...) and that the Australian country has lost 660 million AUD value added across the supply chain network on an overall 2.2 billion AUD losses in value added. Kuhla *et al.* (2021) reveal an economic ripple resonance, which magnifies losses by 21% on average when successive or overlapping weather extremes interact, affecting 1.8 million trade relations between over 7000 regional sectors, with high-income economies experiencing the most significant effects, a critical consideration in assessing past and future economic climate impacts. Moreover, Hallegatte (2008) finds that indirect costs of Hurricane Katrina lead to an increase of the total costs by 39% compared with the direct costs, going from \$107 Billion to \$149 Billion.

Subsequent to the seminal contributions of Hallegatte (2008), considerable progresses have been made. A remarkable improvement is the BoARIO package, a Python-based implementation of the Adaptive Regional Input Output (ARIO) model delineated in Hallegatte (2013), enhanced by the global perspectives introduced by Guan *et al.* (2020). This enhancement incorporates world input-output matrices, now accessible through pymrio, as elaborated by Stadler (2021). Accordingly, this facilitates the adaptation of internal exchanges and the aggregate imports/exports variables, foundational to the approach of Hallegatte (2008), to the global input-output framework, as demonstrated in Table 5. We also present this methodology, illustrate its use and apply it to a real example of a 95% VaR level shock to the US economy.

The last step consists in modeling the impact on asset price and the literature has investigated extreme event impact on several asset classes. For example, commodities response to news related to natural disasters (Marvasti & Lamberte, 2016). Fink *et al.* (2010) focuses on the impact of a particular cyclone on crude oil price index and show that price reactions to storm forecasts are observable within a 24-hour forecast period. Notably, a category 4 hurricane in this area causes an increase in refined petroleum prices compared to crude oil by approximately 13.5%. Kim and Bui (2019) focus on the island ports and supply chain resilience. Energy prices also respond to disasters (Wen *et al.*, 2021).¹

This research paper is organized as follows. Section Two describes the different approaches tackled for Direct damage modeling. Section Three explains how the indirect effects of physical shocks on the economy can be estimated using multi-regional input-output (MRIO) modeling. Section Four introduces the Monte-Carlo simulation we use to calculate the future potential losses due to physical risks. Section Five concludes.

¹Both natural and human extreme events significantly increase oil price risk. Among all natural disasters, the negative impact of an epidemic on oil price risk is the greatest.

Key Findings

Summary

In this paper, we introduce a bottom-up methodology to forecast damages from extreme events to the economy during the 21st century. We model direct and indirect damages using the example of tropical cyclones worldwide and country by country in a top-down fashion with co-occurrence of extreme events and illustrate the distribution of future damages for several countries. We also simulate a 95% VaR magnitude extreme event on the US economy introducing insured damages, impacts and recovery sector by sector.

Results

Under the current modeling assumptions of our framework, an extreme event occurring once every 20 years could come back once every 4 years by 2050 and the average yearly damages from cyclones worldwide might reach 380 billion USD from the current 85 billion USD. Using the example of a 95 % VaR magnitude cyclone on the US economy, losses above 300 billion USD of direct and indirect damages have to be feared, with a significant (40%) part of insured damages and contagions to related sectors (specifically to the financial system).

Insights

This framework can be adapted to tackle a wider variety of physical risks and assess the impact and recoveries throughout the world using regional and sectoral specificities while introducing co-occurrence of extreme events. We should keep in mind the risk of over-fitting our predictions while still supporting strong enough assumptions. No gdp growth assumption is a choice to present more comprehensive results.

2 Direct damage modeling

Currently, there are two primary methods for measuring the damages caused by climate change. The bottom-up approach requires a geolocated cartography of all the physical assets of each company, their sensitivities to the damages related to all disasters, and to aggregate them (first at the company, then at the portfolio level).

To estimate the direct exposure of issuers' facilities this way, we must introduce asset level information and alternative data. On the other hand, the top-down approach generates damages at the sector and country level from past observations and has to model the inheritance of shocks between and within each sector. In both cases, the company direct shock $\mathbb{S}_{k,t}^{(\text{direct})}$ writes:

$$\mathbb{S}_{k,t}^{(\text{direct})} = \frac{\mathcal{A}_{k,t} - \mathcal{D}_{k,t}}{\mathcal{A}_{k,t}} \quad (1)$$

where \mathcal{A}_k is the total asset value of issuer k at year t and \mathcal{D}_k is the value of the damages caused by extreme events at year t .²

2.1 Bottom-up approach: Case of tropical cyclones

In this section, we detail the modeling of company level damages, with the physical impacts of extreme events. We focus on the modeling of tropical cyclones following Le Guenedal and Roncalli (2022).

Hazard intensity We introduce Poisson processes with stochastic intensity $\Lambda(t)$. For each tile (we introduce g to simplify the notation, which initially involves latitude and longitude, such as $X_g \sim X_{lat_5,lon_5,m}$), we represent the number of land-falling cyclones with a counting process:

$$dN_g(t) = \lambda_g(t)dt + dP_g(t), \quad (2)$$

where $dN_g(t)$ is the marginal increment of the counting process for location g , $\lambda_g(t)$ is the stochastic intensity, and $dP_g(t)$ is a Poisson random measure projecting random occurrences of tropical cyclones in future synthetic tracks. Let $\lambda_g(t)$ follow a deterministic drift such as:

$$d\lambda_g(t) = \mu_g dt \quad (3)$$

Thus, for each location on the grid, we can fit the laws based on a large number of future synthetic tracks.³

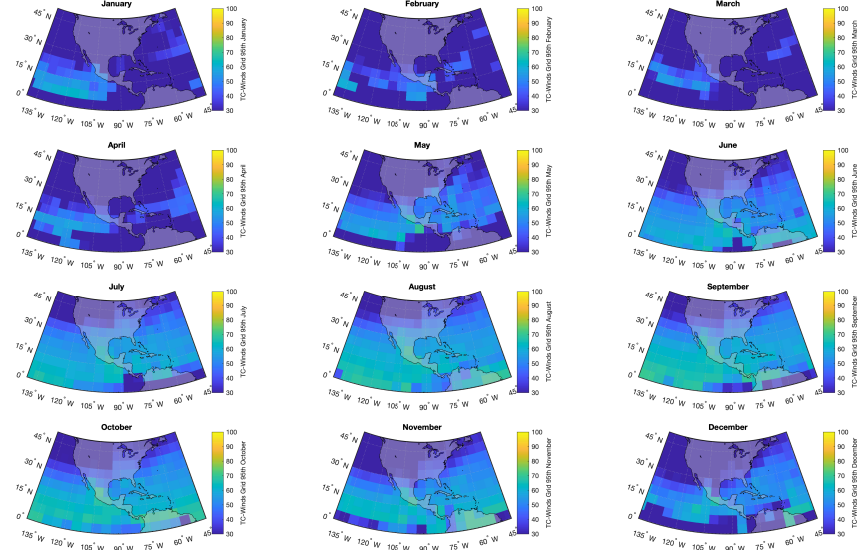
²In what follows we omit the temporal subscript to ease the notation.

³Historical landfalling statistics have been compared over tracks produced with synthetic (Meiler *et al.*, 2022), and changes in log-scale occurrence can be extrapolated as in Bloemendaal *et al.* (2022) or Le Guenedal *et al.* (2022). Future uncertainty in economic impact is also investigated in Meiler *et al.* (2023).

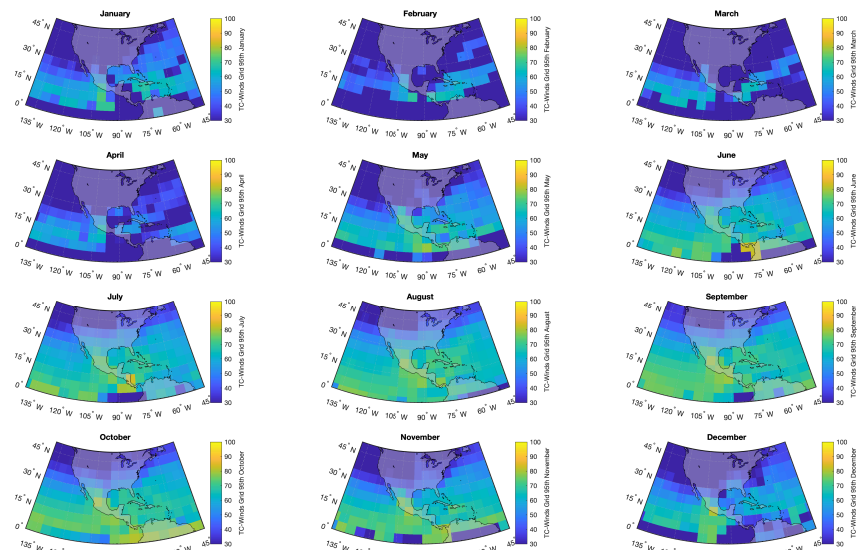
Example of physical modeling: CATHERINA Wind 95th percentile maps

A bottom-up evaluation of damages involves a detailed, granular approach to assess the impact of extreme events, such as natural disasters, on a specific area or infrastructure. The process of building maps to represent the activity of an extreme event is a crucial step in a bottom-up evaluation. For example, results from Le Guenedal *et al.* (2022) allow us to decompose the contribution to shift in tropical cyclones induced damages.

Representative Concentration Pathways 2.6W/m²



Representative Concentration Pathways 8.5W/m²



We reiterate that this illustrative dataset contains 300 representative years with 7 different models on monthly data produced between 2070 and 2100, under the three representative concentration pathways (RCP 2.6, 4.5 and 8.5). From the synthetic tracks generated, one can compute the 95th percentile of maximum wind speeds, which

produces for the RCP 2.6 and 8.5 scenarios W/m^2 in the north American continent the grids above. Thus, we obtain a physical probability - aligned with the concept of value at risk and extreme risks measurement - to obtain a cyclone of each category making landfall each month.

These figures show that there will be enough thermodynamic potential available to lead tropical cyclones to intensify up to Category 5 in the North America by the end of the century using RCP 8.5. We reiterate that CATHERINA makes no assumption on change in initialized disturbances ($\mu_g = 0$ in Equation (3)). Therefore, it maintains very low probability of seeing a cyclone. Refined versions of these maps allow us to produce local Climate Value-at-Risk based on expected losses from the extreme winds.

For each event (cyclone, drought, floods) it is possible to model physically the intensification process. For example for each generated cyclone, it is possible to model precisely the intensification process (depression in the eye), and maximum wind along tracks (Le Guenedal *et al.*, 2022). We can generalize this approach to other disasters.

However, to simplify the process it may be easier to model only highly damaging event (starting with cyclones), and calibrate total damage based on one landfall wind value, generated with stochastic process. The calibration of the Poisson law, guided by the selection of a particular filtration for tropical cyclones (or any specified event), enables the adjustment of the intensity parameter (in the case of tropical cyclones, wind speed). This adjustment aims to align with the aggregated damages produced by the event in various locations. This calibration process facilitates the derivation of pertinent damage distributions and can be executed for individual regions, incorporating numerous hyper-parameters if necessary.

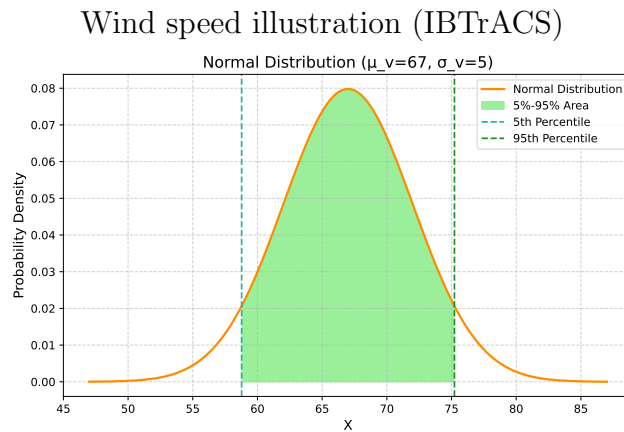
For example, the maximum wind speed for each simulated cyclone can be drawn from a normal distribution, characterized by mean (μ_v) and standard deviation (σ_v), which are derived from historical data on maximum wind speeds of past cyclones. We may for instance, model the landfall wind with a normal distribution of parameters $\mu_v = 67\text{m.s}^{-1}$ and $\sigma_v = 5$ based on the expected wind speed observed on tropical cyclone of this category in IBTrACS.⁴

⁴The International Best Track Archive for Climate Stewardship (IBTrACS) database (Knapp *et al.*, 2010) is available at <http://ibtracs.unca.edu/>.

Modeling Intensity: example of Normal Law for tropical cyclones

In the analysis of extreme meteorological phenomena, particularly cyclones within categories 4 and 5, it is observed that the wind velocities range between 58 and 70 m/s for category 4 and exceed 70 m/s for category 5 cyclones (c.f. IBTrACS). Moreover, category 5 cyclones, which are significantly less frequent than category 4, seldom manifest maximum speeds exceeding 280 km/h (approximately 77 m/s).

In light of this data, it is possible to model wind speeds using a normal distribution with a mean of 67 m/s and a standard deviation of 5 m/s. This parametrization results in the 5th and 95th percentiles of the distribution being approximately 59 m/s and 75 m/s, respectively.



It is important to note that alternative distributions, such as the Weibull or the Generalized Extreme Value (GEV) distribution, are credible alternatives for fits to the observed data.

2.1.1 Local damage functions

In the context of physical risk assessment, we downscale the physical asset value of companies on a grid consistent with hazard models and introduce damage functions. For the latter, in the case of tropical cyclone, we may use the regional damage functions of CLIMADA (Eberenz *et al.*, 2021) - based on Emanuel (2011) generic damage function - introducing temporality handling to account for co-occurrence of extreme events in the same calendar year. Thus, if a second extreme event occurs shortly after a first event, it is likely to impact less structures that have already suffered or are even partially or fully destroyed:

$$f_{r,t}(V, v_h(r)) = \frac{(v_n(V, v_h(r)))^3}{1 + (v_n(V, v_h(r)))^3} \times (\mathbb{1}_{t \in]0; T]} \theta_t + \mathbb{1}_{(t=0) \cup (t > T)}) \quad (4)$$

where $f_{r,t}$ is the fraction of the property value lost in the region r from a cyclone at time t , V is the wind speed and $\theta_t \in]0; T]$ is a multiplier for a damage occurring between 0 excluded, and T when the asset has been fully rebuilt. The second indicator function covers the other cases: $t = 0$ means that no event has ever occurred, while $t > T$ means that the structures

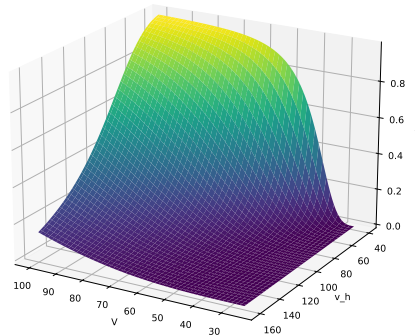
have completely recovered from any previous event.

$$v_n(V, v_h(r)) = \frac{\max(V - v_t(r), 0)}{v_h(r) - v_t(r)}$$

where $v_t = 25.7$ m/s and $v_h(r)$ is a parameter calibrated for each region r . Figure 1 illustrates the sensitivity to v_h and wind parameters. We might find specific scenarios where θ_t is greater than 1, but in practice it is range-bound most of the time.

These damage functions generalize well in terms of asset or event types to other extreme events (wildfire, drought, floods...). The damage functions $f_j(I) \in [0, 1]$ are calibrated using historical records as the fraction of loss of an asset depending on the event intensity I . The appropriate intensity indicator is different for each event and all kinds of storms, while damages are generally correlated to maximum wind speeds ($m.s^{-1}$) with a threshold or central pressure (hPa). For floods, flood depth (m) is commonly used (Huizinga *et al.*, 2017). Used indicators may vary for the different sectors and a single event: for instance, for droughts, standard precipitation index and evaporation are likely to affect energy sectors while the maximum number of consecutive frost/wet or dry days and diurnal temperature among other agro-climatic indicators are more appropriate for the agriculture sector.

Figure 1: Fraction loss function in terms of the values of v_h and V (Emanuel, 2011)



2.1.2 Asset exposure

To measure the exposure of specific companies to natural hazards we must introduce geolocated information about corporate facilities. A first estimate, that is relevant at the country level, is the LitPop (Eberenz *et al.*, 2020) dataset downscaling the GDP on a map. Other sources, with thinner sectoral granularity are increasingly available (see Example Box). In this paper, we do not introduce geolocated assets nor use sector geo-referenced activity, but present the theoretical foundation of the method that rely on this data.⁵

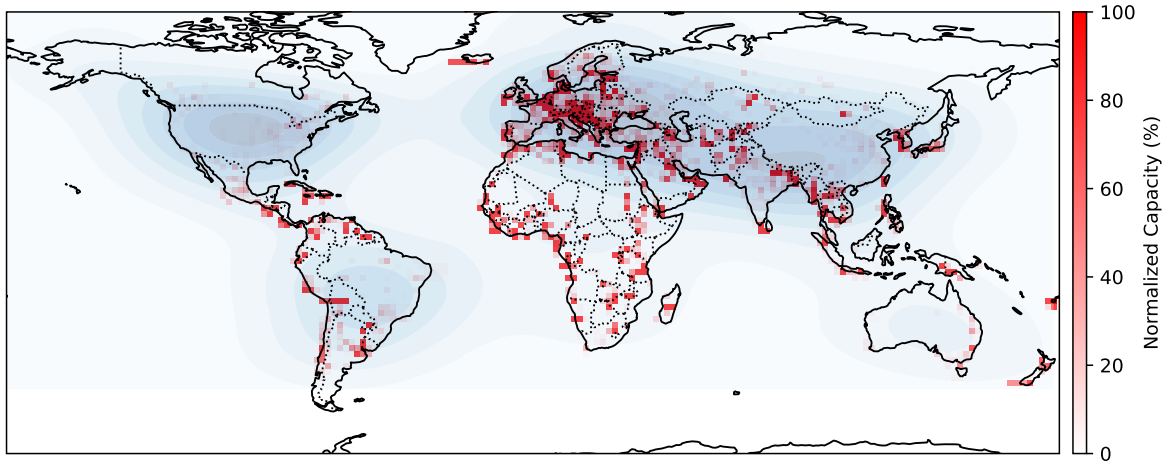
⁵Our empirical illustration rely on the top-town approach presented section 2.2 implemented in a monte-carlo (section 4).

Definition of an exposure metric Let us introduce the density measure γ_g^k and fraction Γ_r^k that denotes respectively the probability of presence of a company in a tile, and its fraction of revenue in a country. We thus make the assumption that the total physical asset of a company is distributed similarly as its revenue split (Le Guenedal *et al.*, 2023). For each company k , summing over the grid within a country sums to the total revenue share allocated in this country, $\sum_{g \in r} \gamma_g^r = \Gamma_r^k$ and $\sum_r \Gamma_r^i = 1$. The rationale of this metric is to construct a density map of the area to which the company k is sensitive to. This density based approach can be modeled at the sector level or asset level depending on the data source used. For example, using news data can help building density at the company level. Some open-source datasets can be used to build sectoral densities.

Examples of construction of exposure indicators the power and commodities sectors from open-source data

Example A. The Global Power Plant Database (GPPD) is a comprehensive and open-source database of power plants worldwide. It serves as a centralized repository of power plant data, making it easier to navigate, compare, and draw insights for analysis. The database covers approximately 35,000 power plants from 167 countries, including both thermal plants (such as coal, gas, oil, nuclear, biomass, waste, and geothermal) and renewables (such as hydro, wind, and solar). Each power plant is geolocated, and entries contain information on plant capacity, generation, ownership, and fuel type.^a

Normalized power sector capacity (per country) based on GPPD

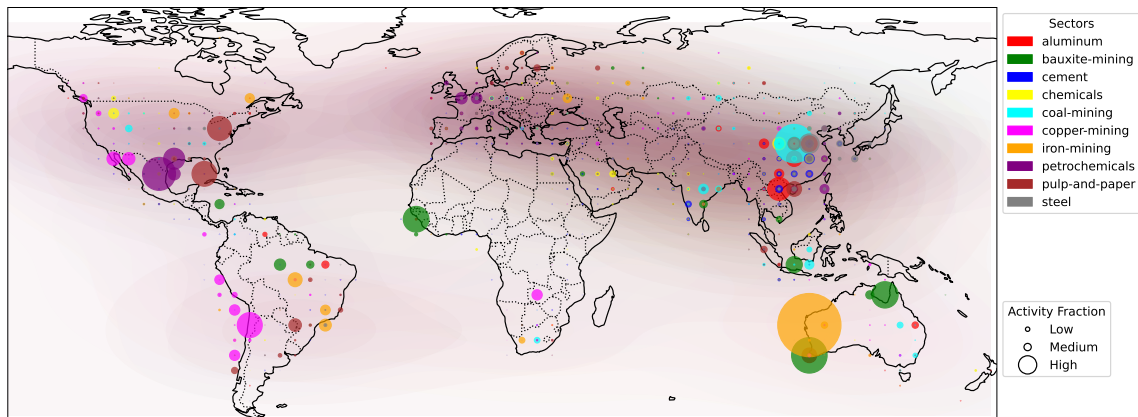


From this dataset, we illustrate the construction of a density measure $\gamma_{g,r}$ that denotes the probability of presence of an energy facility on the tile g and in the country r .

In this illustration, we compute the total production capacity (MW) of the power plants in one country and normalize the capacity of each tile g by the total capacity of the corresponding country. Then, we highlight the tiles where a large proportion ($\gamma_g > 20\%$) of the country's capacity is located. These values represent the local exposure of the energy sector worldwide. We can extend it including measures for other sectors.

Example B: Illustration of commodities from the Climate Trace (Tracking Real-time Atmospheric Carbon Emissions) database represents an innovative approach to monitoring greenhouse gas (GHG) emissions across various sectors worldwide. This initiative is particularly important for understanding, managing, and reducing emissions in a detailed and timely manner. The database leverages advanced technologies, including artificial intelligence (AI), satellite imagery, and remote sensing data, to provide an unprecedented level of transparency and accuracy in tracking emissions. Here is a world map overlaid with various colored circles, each representing the concentration of different industrial sectors: Aluminum, Bauxite, Cement, Coal, Copper, Iron, Petrochemical, Pulp and Paper and Steel. The capacities are grouped on a five degree grid (latitude and longitude) and the geolocated sources with missing capacity are ignored in this visualization.

Normalized commodities capacity (per country) based on Climate Trace



The circles are concentrated in areas that are presumably major hubs for these industries. The size of the circles seems to indicate the level of activity of each sector. Large circles indicate high activity fraction in that sector reported in climate trace databases and small circles indicate lower reported activity. It reflects the global distribution of various industrial sectors based on our understanding of these industries.

Concerning aluminum, China remains the largest producer of alumina and primary aluminum, accounting for almost 60% of global production in 2022.^b Aluminum production is closely linked to the availability of bauxite ore, which is primarily found in tropical and subtropical regions. The chart shows significant activity in regions known for bauxite mining, such as Australia and South America. Steel production is typically found in industrial regions with access to iron ore and coal. The map shows high activity in traditional steel-producing regions such as China, Europe, and North America.

Cement manufacturing is a widespread industry essential for construction, one can find broadly in every country. The map indicates activity in various global locations, which aligns with the widespread nature of the construction sector. The chemical industry is diverse and can also be found worldwide due to the broad range of products it

encompasses. It is often located near oil and gas reserves or in industrial hubs, as put on evidence by the map.

It indicates high activity in regions known for coal reserves, such as parts of China, the United States, and Australia, which are some of the world’s largest coal producers. Global coal trade volumes hit record levels in 2023, but are expected to decline in subsequent years. The market dynamics are largely influenced by Asia’s growing presence, with China and India set to account for over 70% of global coal consumption by 2026.

Significant copper mining activity is shown in areas known for copper resources, like parts of South America (Chile and Peru) and Africa (the Democratic Republic of Congo and Zambia). The map shows activity in regions renowned for iron ore production, such as Western Australia, Brazil, and parts of China and Russia. The petrochemical industry is often located near oil and gas fields or refineries. The map reflects this with high activity indicated in the Middle East, the United States (Gulf Coast), and parts of Asia. The Pulp and Paper industry is usually found in regions with abundant forest resources, and the map shows activity in corresponding areas like Northern Europe, North America, and parts of South America.

Overall, the distribution of sectors on the map aligns with known global patterns of industrial activity. However, the exact relevance would also depend on the data sources, date of the information, and accuracy of the representation. The map provides a snapshot that could be useful for insights into global industrial patterns, resource allocation, and potential environmental impacts.

^aThe database will be continuously updated as new data becomes available. The methodology for creating the dataset is detailed in the World Resources Institute publication ‘*A Global Database of Power Plants*’.

^bInformation about Aluminum can be found here: <https://www.iea.org/energy-system/industry/aluminium>.

Total asset value losses Once the asset exposition maps have been constructed, we can sum up the losses from the simulated event to compute future expected losses for company i of total assets \mathcal{A}_k :

$$\mathcal{D}_k = \mathcal{A}_k \times \sum_g \sum_{N_g} \gamma_g^k \times f_{r \ni g}(\hat{V}^{N_g}, v_h(r)) \quad (5)$$

To compute the total loss at the sector \times country level ξ_i , we must sum the losses over the issuers. It follows that the sectoral shock writes:

$$\xi_i = \sum_{k \in i} \frac{\mathcal{M}_k \times \mathcal{S}_{k,t}}{\mathcal{M}_i} \quad (6)$$

where $\mathcal{M}_{i,k}$ are respectively the market capitalization of the sector i and company k (which allow to account for company size in the transmission of the shock). Alternatively, enterprise value could be used here, as there are cases where the company cash flows are being used to cover the losses, all else being equal, and as the impacts on market capitalization of an extreme event are often very uncertain. Assuming that this physical shock (on total

physical assets) is transmitted proportionally to each financial asset, it allows to compute direct physical shocks on an investment portfolio in a bottom-up fashion.

Note that we often illustrate the framework with tropical cyclones, but the approach is generalizable to other disasters. Poisson laws (and drift) have to be generated for each disaster, in each area. In this paper, we decided to rely on the top-down modeling of direct shock, presented hereafter, thus we did not conducted the thorough calibration of generation laws, climate sensitivity and damage functions for each type of extreme events and assets.

2.2 Top-down approach: stochastic shock matrix

2.2.1 Modeling occurrences of extreme events

We can express the number of extreme events in country r with a counting process:

$$dN_r(t) = \lambda_r(t)dt + dP_r(t)$$

The main difference is that the number of shocks is defined at the country level, while it was specified locally in the previous section. We can even simplify:

$$N_r(t) \sim \mathcal{P}(\lambda_r)$$

where λ_r will be evaluated using historical events data. The time dependence will be pushed in the shock rather than in the number of events per year, knowing that the model links linearly the fraction loss and the number of events. To estimate the value of λ_r we count the extreme events that have occurred in the world between 2000 and 2024 with the EM-DAT data which classifies all the natural and technological disasters from 1900.⁶

In this paper, we account only for events with damage costs above 1\$ Bn or representing more than 1% of the GDP of the impacted country (from the World Bank Data⁷) since 2000. Furthermore, we focus on extreme events which frequency and intensity are directly impacted by climate change. Thus, we include floods, storms (tropical and extra-tropical), extreme temperatures / heatwaves, droughts or wildfires, still modeling the specific case of tropical cyclones in this paper. We count overall 376 extreme events in the world. Those disasters are distributed in the different regions as described in Table 1.⁸

2.2.2 Downscaling of the shocks

For each country, we decompose the losses at the sector-level. We also consider that multiple countries may experience concurrent impacts within a single year. To take this into account, we introduce stochastically the function of direct losses and for each time define the diagonal sparse matrix (of same dimension than A the input-output matrix):

$$S^{\text{diag}} = \begin{bmatrix} \xi_{1r} & 0 & \cdots & 0 \\ 0 & \xi_{2r} & \cdots & 0 \\ \vdots & \vdots & \ddots & \vdots \\ 0 & 0 & \cdots & \xi_{nr} \end{bmatrix}$$

⁶available at: <https://public.emdat.be/>.

⁷available at: <https://data.worldbank.org/>.

⁸See Table 10 in Appendix for more details.

Table 1: Statistics of damages and frequencies of extreme events per region

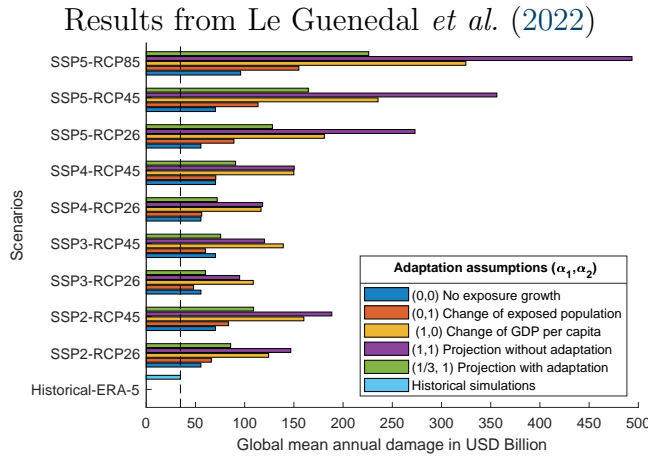
	Number	Freq λ_r per year	Mean Total Dam (\$Bn)	Std of Total Damage (\$Bn)
Africa	9	0.38	1.158	1.894
Americas	228	9.5	6.495	18.458
Asia	86	3.58	3.579	3.758
Europe	27	1.13	2.160	1.860
Oceania	26	1.08	1.145	1.224
Overall	376	15.67	5.019	14.630

where ξ_{ii} are the damage functions (defined formally in the next paragraph), $\frac{\mathcal{D}_{i,r}}{GDP_{i,r}}$ are the simulated damages for sectors i in country r at time t , $\mathcal{C}_{SSP-RCP}$ is the mean coefficient of increase of direct damages for each SSP-RCP scenarios. As in previous section, $\mathcal{D}_{i,r}$ can be adjusted depending on the proximity of occurrence of the event as regards previous events.

The increasing occurrence of extreme events with climate change must be calibrated externally, globally or locally, ideally for each event type. In this exercise, we illustrate the functioning of our framework with a simple linear parameter retrieved from the CATHERINA model. Thus, we use the value for $\mathcal{C}_{SSP-RCP}$ associated to the SSP 5-RCP 8.5 (without growth in exposure). This would correspond approximately to an annual increase of 4% between 2020 and 2070 (see Example Box below). Note that the increase of damages and their occurrence through time can be extended to all kinds of extreme events. They however require precise calibration and data, and are not the purpose of this paper.

Example of annualized regional damage increase modeling

In CATHERINA, Le Guenedal *et al.* (2022) introduce physical asset value from Eberenz *et al.* (2019, 2020) and project it on the SSPs to simulate damage induced by synthetic tracks.

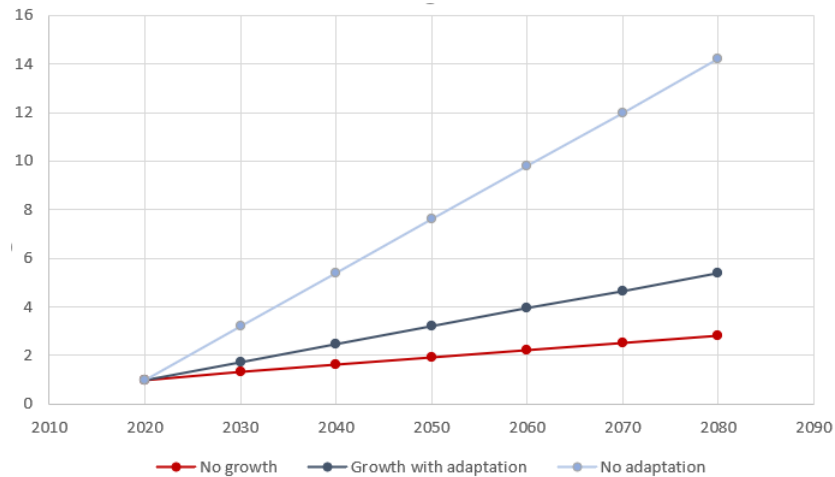


One can use directly the global output of this model to compute change in cyclone-related damage exposure at the country level.^a We reiterate the final results suggested by the model (Le Guenedal *et al.*, 2022). Above, the expected value of global annual

damage (in USD billion) in different SSP-RCP and exposure projection hypothesis configurations can be found. Adaptation assumptions have a huge impact on the rate of growth of cyclone-related damages to the economy. For example the SSP 5-RCP 8.5 scenario under no exposure growth assumption (upper blue bar, 100 billion \$ mean annual damage) presents lower mean annual damages at the horizon 2070 than SS 2-RCP 2.6 with no adaptation (lower purple bar, 150 billion \$ mean annual damage).

It illustrates the estimation of annualized damage increase in the hottest scenario (RCP 8.5) and the fossil-fueled development shared socioeconomic pathways (SSP 5) while we only consider the increase of damages induced by global warming. It means that we do not acknowledge for the rise of GDP per capita or population. With these assumptions, the average damages is to be tripled by 2070/80^b (Le Guenedal *et al.*, 2022). The evolution in time of extreme event intensity may be based on CATHERINA model, and similar works, calibrating $\mathcal{C}_{SSP-RCP}$ on the results.

Example of linearization of the damage growth suggested in Le Guenedal *et al.* (2022)



We may suppose that this increase is distributed linearly and independently of the region, namely that each year we have the same rise of losses of approximately 4%. Thus the mean coefficient of increase of damages of extreme events due to climate change at annual step $\hat{t} = t - 2020$ be:

$$\mathcal{C}_{SSP-RCP}(t) = 0.04 \times \hat{t}$$

Note that an exponential rate of growth remains very credible.

^aOther papers such as Meiler *et al.* (2023), also explore the changes in future exposure and economic impact of tropical cyclones.

^bUnder the assumption of no future adaptation, the RCP 2.6 scenario, consistent with the Paris Agreement aiming to keep global warming below 2°C by 2100, forecasts a quadrupling (factor of 4.2) of the expected global annual financial losses from tropical cyclones over the 2070-2100 period. Under the conservative assumption of no exposure growth, for the RCP 8.5 scenario, ignoring changes in GDP per capita and population, the expected damage would still grow by a factor of 2.8. Supposing that the damages grow evenly per year we have the following rate of increase: $\frac{2.8-1}{2070-2020} \sim 4\%$

This approach requires to introduce hazard and country specific damage functions. In line with remark 2.1.1, we reiterate that each hazard has a different measure of intensity (flood depth (m), consecutive dry days without precipitation (days), wind speed (m/s), etc.) and each country, sector, or even at a more granular level facility, has different damage curves. In the context of global portfolio assessment, we choose to rely on an empirical approach simulating directly the damages based on past observations.

2.2.3 Top-down damage function

To model the distribution of extreme event damages in terms of fraction of GDP, we use a log-normal law⁹ approach as commonly used in statistical modeling to capture the positiveness and right-skewness of losses, and introducing a representation of the reduction of damages within relatively short successions of events, and a penalty coefficient to embody the different sensitivities of each sector to the extreme event:

$$\xi_{i,r,t} = N_r \times \mathcal{LN}(\mu_r, \sigma_r) \times (1 + \mathcal{C}_{SSP-RCP}(t))^t \times (\mathbb{1}_{t \in]0;T]} \theta_t + \mathbb{1}_{(t=0) \cup (t>T)}) \times \rho_i \quad (7)$$

where μ_r and σ_r are parameters accounting for the intensity of damages calibrated using historical data in the EMDAT database, $\theta_t \in]0;T]$ is a multiplier for a damage occurring between 0 excluded, and T when the asset has been fully rebuilt. The second indicator function covers the other cases: $t=0$ means that no event has ever occurred, while $t > T$ means that the structures have completely recovered from any previous event. Finally, ρ_i is a multiplier of the damages related to industry i as we do not expect the damages to be evenly distributed across sectors. It follows a $\beta_{(\alpha_i, \beta_i)}$ law.

We first, compute the mean μ_e and standard deviation σ_e of the damages of the observed extreme events in percent of GDP. We then use the following formulas between the log-normal parameters and the expected mean and standard deviation:

$$\begin{cases} \mu = \ln\left(\frac{\mu_e^2}{\sqrt{\mu_e^2 + \sigma_e^2}}\right) \\ \sigma^2 = \ln\left(1 + \frac{\sigma_e^2}{\mu_e^2}\right) \end{cases}$$

Table 10 shows that extreme events cause a loss of 5.21 \$Bn in average between 2000 and 2017, with standard deviation of 12.54 \$Bn. In terms of percent of GDP of the countries affected it comes to 3.35% of mean damages and 0.144 of standard deviation. We calibrate μ and σ^2 according to the following table to take into account the disparities between countries.

These figures present the main countries that have been affected by extreme events over the past 24 years, and the corresponding calibration of μ and σ for the log-normal law. These parameters are used in the simulation procedure in section 4.

⁹The use of log-normal or power laws is discussed in Blackwell (2015) in the context of damages of American hurricanes between 1900 and 2005

Table 2: Regional calibration of μ and σ

Country	μ	σ
Australia	-5.901	0.115
China Mainland	-7.502	0.167
France	-5.16	0.105
India	-5.438	0.145
Japan	-6.513	1.266
Mexico	-4.397	0.128
United States of America	-7.817	1.868

Calibration of sectoral damages: case of tropical cyclones

Using the empirical evidence from Debbie Tropical Cyclone (2017) brought by Lenzen *et al.* (2019), we can determine the parameters $\mu_{i,r}$ and $\sigma_{i,r}$ describing the fraction loss in terms of the different sectors and regions. We reproduced in Annex Table 7 the fraction losses for Australian sectors after Debbie. We also need to take into account the vulnerability of each region. To do so we use a vulnerability parameter $v_h(r)$ which describes the speed of wind that generates a fraction loss of 50% in the region r . This parameter is cataloged in Table 13 using CLIMADA model from Eberenz *et al.* (2021).

Using the values of $\xi_{i,Aus}$ from the Table 7 and the values of $v_h(r)$ in Table 13 we can find the standard deviation of each country and sector. Let σ be the standard deviation of all the non-null values of sectorial fraction loss from Debbie Tropical Cyclone, we choose:

$$\begin{cases} \sigma_{i,r} = \sigma = 0.093 & \text{for every region } r, \text{ if sector } i \text{ highly relies on physical assets} \\ \sigma_{i,r} = \frac{1}{2} \times \sigma & \text{for every region } r, \text{ if sector } i \text{ does not rely on physical assets} \end{cases}$$

Indeed, averaging non zero damages for every region in Australia gives us that agriculture related sectors (highly reliant on physical assets) lead the damages fraction with about 17%, followed by accommodations (6.7%) and energy (6.2%), while transports, trades, construction and health, although impacted, present lower coefficients. The choice of coefficients presented by the authors is chosen so as to generalize as well as possible to different kind of events.

As for μ we will be considering that it is null for non-affected sectors in all regions and otherwise that it can be retrieved from the Equation (4) and that:

$$\mu_{i,r} = f_r(V, v_h(r))$$

where V is the speed of the tropical cyclone and $v_h(r)$ the vulnerability parameter of the region r . The evolution of the fraction loss (or μ) function is depicted in the Figure 1.

3 Modeling indirect effects of physical shocks

In this section, we provide a technical review of the literature summarizing approaches of the diffusion models allowing to represent the propagation of shocks to the economy that are based on input-output frameworks.

When an extreme event occurs, the immediate damage to each sector/country induces damages to the sectors linked to the initial sector. For example, if a cyclone impacts the United States with losses to the agriculture sector, it will impact its instantaneous production and production capacity, which in turn will impact the production of the sectors dependent on the agriculture sector, both regionally and internationally. Prices, demand, rebuilding demand, employment and inventories are also likely to be significantly modified. The diffusion coefficient to each economy is both based on the resilience of each sector (capacity to overproduce) and the interconnection between the sectors (input-output tables).

Proper modeling is of highest concern for many actors of the economy as reported damages related to extreme events occurrence (and temporal dynamics) usually only concern direct effects and a very small part of the indirect damages. We illustrate some case studies with examples and corresponding computations.

3.1 Classical input-output diffusion through sector requirements

The physical damages could impact the value-added in a similar way to transition risks, as described in Desnos *et al.* (2023). However, there is a key difference: we expect physical risk to be more locally concentrated. We model this difference as a constant factor that modifies the impact of physical damages. Considering a flexible price model:

$$p_j = \sum_{i=1}^n A_{i,j} p_i + v_j + \mathbb{S}_{\text{direct}} \quad (8)$$

where $A = (A_{i,j})$ is the input-output matrix, p_j is the price of sector j , v_j is the added-value of the sector j and $\mathbb{S}_{\text{direct}}$ is the direct shock rate vector. Thus:

$$\begin{aligned} p &= \left(I_n - A^\top \right)^{-1} (v + \mathbb{S}_{\text{direct}}) \\ \implies \Delta p &= \left(I_n - A^\top \right)^{-1} \mathbb{S}_{\text{direct}} \end{aligned} \quad (9)$$

$$\begin{aligned} \mathbb{S}_{\text{indirect}} &= \Delta p \\ &= \left(I_n - A^\top \right)^{-1} \mathbb{S}_{\text{direct}} \end{aligned}$$

The total shock on the different sectors is:

$$\begin{aligned} \mathbb{S}_{\text{total}} &= \mathbb{S}_{\text{direct}} + \mathbb{S}_{\text{indirect}} \\ &= \mathbb{S}_{\text{direct}} + \left(I_n - A^\top \right)^{-1} \mathbb{S}_{\text{direct}} \end{aligned} \quad (10)$$

And we can then multiply by the global output to get the total loss on the economy:

$$S_{\text{total loss}} = x \odot (S_{\text{direct}} + S_{\text{indirect}}) \quad (11)$$

Here, there is a strong assumption that the price of the damage caused by the disaster will be passed on the output prices. In practice, it may not be that simple for numerous reasons: First, costs of damages may not have the same pass-through (if there is any) as a carbon tax as it is presented in Desnos *et al.* (2023). Unlike a taxation like the carbon tax that is supposed homogeneous in Desnos *et al.* (2023) — where the incidence falls relatively uniformly across sectors and worldwide and thus does not perturb the relative competitiveness (in case of global carbon pricing) — the pass-through of idiosyncratic damages is more uncertain.

A tax has the potential to be fully transmitted onto prices in a manner that is sector-agnostic, preserving inter-sectoral competitive equilibrium. On the contrary, localized damages bring out an asymmetric shock to the cost structure of affected entities, which are constrained by the elasticity of demand and the price-setting strategies of competitors. In other terms, if a steel manufacturer loses physical capital, it may not be able to shift-up the price of steel because competitors may not have faced extreme events. Therefore, while a tax could theoretically result in a neutral shift in the supply curve across industries, disaster damages may not. Affected firms are likely to face a competitive disutility if they attempt to pass these costs onto consumers, given the heterogeneity of the shock and the competitive ceiling on price increases. These heterogeneous conditions can lead to credit stress, as the damaged sectors may not be able to adjust their prices proportionately without eroding their market positions.

Conversely, a temporal concentration of extreme events — multiple incidents within a narrow time frame, such as a single calendar year — could catalyze systemic economic stress. This confluence can induce an anxiety-propelled escalation in the prices of key commodities, potentially exceeding the tangible costs of damages incurred. This inflationary effect goes beyond the direct impact of the events to reflect the market’s response to perceived scarcity, heightened risk aversion, and anticipatory behaviors associated with securing resources against future disruptions. The resulting price inflation thus embodies not only the actualized costs but also a behavioral risk premium born from collective market trepidation.

For extreme shocks on some particular strategic sectors that are not present in many regions (e.g. semiconductor in Taiwan), the disruption of the supply-chain may have even higher costs. This can be seen as well for businesses with a strong dependence. In general, the sectors most impacted by extreme weather like tropical cyclones, are sectors with strong reliance on physical infrastructures, for example, mining and materials, fossil fuel and pipelines, manufactures and heavy industries, and utilities. These industries often benefit from quasi-monopolistic status allowing them to pass most of the input costs into their products.

Nevertheless, we make the reasonable assumption in this paper that direct physical losses translate to output prices through common mechanisms. Therefore, we adapt Desnos *et al.* (2023) to include a constant, multiplier of the losses. An alternative would be to impact more strongly local markets via the adaptation of the pass-through rate.

Example 1: Illustration of the direct shock diffusion

Let us introduce an example decomposing the Australian economy into four different sectors: *Energy*, *Agriculture*, *Industries* and *Services*. Taking the following random Input-Output matrix, value-added and output:

Sector	A				x
Energy	0.22	0.4	0.16	0.01	171
Agriculture	0.15	0.35	0.12	0.2	146
Industries	0.1	0.15	0.15	0.11	82
Services	0.45	0.1	0.25	0.1	171
Value added	35	12	20	50	
Income	50	40	8	32	

Thus, the Leontiev matrix can be expressed as:

$$\mathcal{L} = (I_4 - A^T)^{-1} = \begin{pmatrix} 1.8613 & 0.8889 & 0.5280 & 1.1761 \\ 1.3601 & 2.3358 & 0.7197 & 1.1395 \\ 0.6611 & 0.6770 & 1.4794 & 0.8167 \\ 0.4037 & 0.6117 & 0.3466 & 1.4772 \end{pmatrix}$$

and the production vector is:

$$x = \begin{pmatrix} 171 \\ 146 \\ 82 \\ 171 \end{pmatrix}$$

We also compute the vector v of value added ratios:

$$v = \begin{pmatrix} 35/171 \\ 12/146 \\ 20/82 \\ 50/171 \end{pmatrix} = \begin{pmatrix} 0.21 \\ 0.08 \\ 0.24 \\ 0.29 \end{pmatrix}$$

First, we note that $\mathcal{L}v = p^- = \mathbf{1}_4$, meaning that the prices pre-disaster are standardized and equal to one.

In this framework, we can introduce a tropical cyclone (with similar consequences than Debbie), causing direct losses of 30% of the agriculture sector, 10% of the industrial sector, 20% of the energy sector and 10% of the services. It leads to the direct losses vector:

$$S_{\text{direct}} = x \odot \begin{pmatrix} 0.2 \\ 0.3 \\ 0.1 \\ 0.1 \end{pmatrix} = \begin{pmatrix} 34 \\ 44 \\ 8 \\ 17 \end{pmatrix}$$

Therefore, Equation (9) gives us post disaster prices:

$$\begin{aligned}
 p &= \mathcal{L}(v + S_D) \\
 &= \begin{pmatrix} 1.8613 & 0.8889 & 0.5280 & 1.1761 \\ 1.3601 & 2.3358 & 0.7197 & 1.1395 \\ 0.6611 & 0.6770 & 1.4794 & 0.8167 \\ 0.4037 & 0.6117 & 0.3466 & 1.4772 \end{pmatrix} \begin{pmatrix} 0.41 \\ 0.38 \\ 0.34 \\ 0.39 \end{pmatrix} \\
 &= \begin{pmatrix} 1.7375 \\ 2.1393 \\ 1.3563 \\ 1.0967 \end{pmatrix} \\
 \text{Indirect loss is: } \mathbb{S}_{\text{indirect}} &= x \odot \begin{pmatrix} 0.74 \\ 1.14 \\ 0.36 \\ 0.10 \end{pmatrix} = \begin{pmatrix} 126 \\ 166 \\ 29 \\ 17 \end{pmatrix}
 \end{aligned}$$

Thus, the total shock is:

$$\mathbb{S}_{\text{total loss}} = \mathbb{S}_{\text{direct loss}} + \mathbb{S}_{\text{indirect loss}} = \begin{pmatrix} 160 \\ 210 \\ 37 \\ 34 \end{pmatrix}$$

meaning that indirect shocks represent on average more than 70 % of the total shock experienced due to the disaster. For example, as Debbie caused AUS 3.5 billion \$ of direct damages, this would imply additional damage of AUS 8.1 billion \$. In practice, total reported damage may also already account for a part of the indirect shocks.

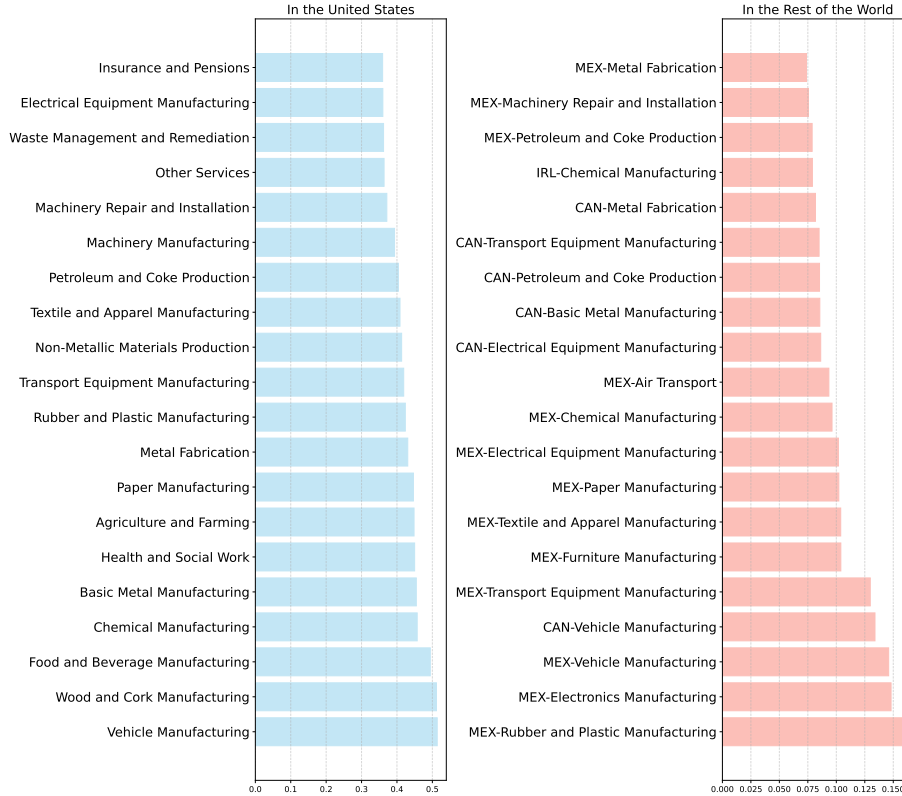
To account for global diffusion of extreme event shocks, we introduce a multi-regional input-output database and illustrate the impacts of applying a uniform direct shock rate of 20% to the United States of America and Australia. This amount is well above any historical record for these two countries and is used for illustrative purpose only to measure the diffusion effect. The 20 internal and external sectors whose prices were most affected by both disasters are illustrated in Figure 2 for the USA (and Figure 12 in the Appendix for Australia).

We observe on the Figure 2 that the sectors most affected by the diffusion of a shock in the US are located in Mexico and Canada for all but one and that those sectors are mostly vehicle or transport equipment manufacturing, petroleum, chemicals, metal or other manufacturing overall sectors. As a matter of fact, according to the United States Census Bureau¹⁰ the first two locations of American exportation are Canada first and Mexico second, respectively accounting for 17.6% and 16.6% of the US total exports. Furthermore, according to the Sherbrooke University¹¹ figures, in 2015, manufactured products represented 75% of the

¹⁰<https://www.census.gov/>, last visited in

¹¹<https://perspective.usherbrooke.ca/bilan/servlet/BMImportExportPays?codePays=USA>, last visited in

Figure 2: Illustration of price dynamics sector per sector after the American disaster



exportations of the United States within mostly metals, chemicals, transport and machinery equipments. Petroleum is also highly exported. Overall the sectors and regions affected using this method both make sense. (See also Figure 13 for the links between Australia and the 10 most affected countries).

Figure 12 shows that the most affected sectors by second round impact of tropical cyclones hitting Australia are located in Taiwan, Japan, India, Malta, Korea (South), China, the Netherlands, Bulgaria or the United Kingdom and are mostly metal or metal manufacturing sectors such as ‘basic metal manufacturing’ and other kinds of manufacturing such as machinery. It makes sense, indeed, according to the Observatory of Economic Complexity¹², the top exports of Australia are metal related sectors and industrial machinery and the most places where it exports are China, Japan, South Korea and India. Thus, there is a clear link between the top exportation sectors and countries and the countries and sectors where the difference of price is the highest after a potential Australian disaster.

We then compare the internal and external diffusion for both the Australian and American disaster. To do so, we consider extreme cases (e.g. ‘*worse case scenario*’) with direct damages in the US of 20% of the production (e.g. $0.2 \cdot x$) and the indirect damages are $\Delta p \cdot x$. The direct damages in the rest of the world are null and the indirect damages are defined similarly. This way, we are able to compute the value of indirect damages per sector and country and also the value and distribution of direct and indirect damages internally to the

¹²<https://oec.world/en/profile/country/aus>, last visited in

US. The following table compares the overall diffusion of the shock either in Australia or in the US on the concerned country and on the rest of the world using the following metrics:

$$\text{Amplification ratio} = \frac{\text{Indirect Damages} + \text{Direct damages}}{\text{Direct Damages}} - 1$$

The results are illustrated Table 3. We note that a direct and indirect total shock in the USA affecting 20% of the production would lead to impact up to 7 trillion \$ with indirect impact on the rest of the world of 1 trillion \$. On the other hand, the same fraction loss in Australia would lead to a direct impact of 1 trillion \$ for 217 billion \$ of indirect losses.

Table 3: Diffusion of the direct shock in the USA and in Australia after a disaster

		Total damages (USD billion)	Amplification ratio
United States of America	Internal	7 204.3	67.4 %
	ROW*	1 089.9	15.1 %
-----		-----	-----
Australia	Internal	1 366.7	73.8 %
	ROW	217.2	43.5 %

Notes: * Rest of the world is computed aggregating all the countries in Exiobase external to the country impacted.

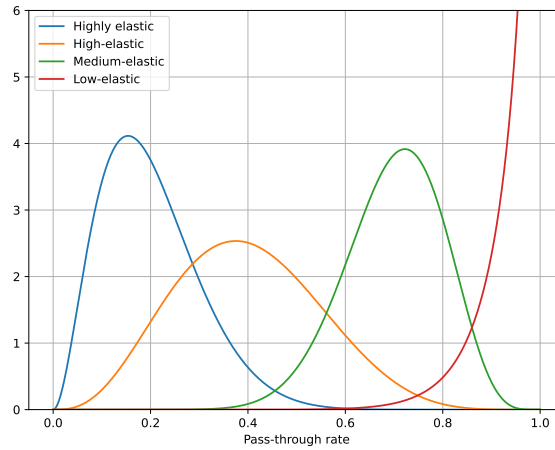
Pass-through rate Unlike for transition risk and carbon price diffusion, there is less literature on the fraction of total physical damage and repair costs cascading in the supply-chain. We can however intuit a similar mechanism (under certain competition assumptions) and introduce a pass-through rate ϕ , which depicts how much of the direct losses suffered by a sector will be passed onto the prices and thus impact other sectors. As discussed earlier, we add a modifying constant c to this pass-through rate to take into account the more "local" diffusion of an extreme event in average. This variable ranges from 0%, meaning that there is no diffusion and each industry bears the full losses, to 100% meaning that all the losses are passed onto the prices. The general formula is as followed (Desnos *et al.*, 2023):

$$\phi = \frac{dp}{d\tau} = \frac{\text{price sensitivity of supply}}{\text{price sensitivity of supply} - \text{price sensitivity of demand}} \times c \quad (12)$$

and for each sector i it can be simplified this way:

$$\phi_i = \frac{1}{1 - \frac{\text{price-demand elasticity of sector } i}{\text{price-supply elasticity of sector } i}} \times c \quad (13)$$

The pass-through rate is highly dependent on the economic situation of the sector we consider; it can be lower than 50% only in perfect competition settings. Otherwise it is always greater than 50% and can even be greater than 100% if the demand is highly convex (Desnos *et al.*, 2023), even if the situation is unlikely in practice. Knowing that the pass-through

Figure 3: Standard probability distribution of pass-through rates from Desnos *et al.* (2023)


rate exclusively depends on price elasticity, we can use the figures and modeling used for the carbon tax pass-through rate from Desnos *et al.* (2023) modulo a constant c .

It is described in Desnos *et al.* (2023) that the pass-through rate follows a Beta law $\beta(\alpha, \beta)$ whose parameters can be found either using a method of maximum likelihood or a method of moment. The Table 9 which describes the probabilistic parameters of the law in function of the four sector's price elasticity can be found in annex as well as the distribution of the different sectors to the different levels of elasticity (Table 8). The probability distribution of those pass-through rates is found in Figure 3.

Replacing in 10, we get:

$$\begin{aligned} \mathbb{S}_{\text{total}} &= \mathbb{S}_{\text{direct}} + \mathbb{S}_{\text{indirect}} \\ &= \mathbb{S}_{\text{direct}} + \phi \times \left(I_n - A^\top \right)^{-1} \mathbb{S}_{\text{direct}} \end{aligned} \quad (14)$$

The modeling of pass-through rates using Beta laws allows us to introduce some non-linearity in the relationship between output prices, shocks and value-added.

Remark 1 *West and Jackson (2004) have introduced another non-linear representation of input-output modeling with application to regional impacts of tourism on Australian economy. The delta in prices is being introduced as:*

$$\Delta p = (I_n - A^\top)^{-1} (\Delta \hat{W} + \Delta \hat{O} + \Delta \hat{M}) (\hat{X}_0^{-1}) i \quad (15)$$

where W is the vector of household income flows by industry, O the vector of other value added by industry (that could be integrated in our framework as idiosyncratic shocks to the economy that are neither from direct nor indirect origin), and M the vector of competitive imports by industry.

3.2 Optimal production after extreme events

Steenge and Bočkarjova (2007) proposed an approach accounting for the labor. The model starts from the standard economic open model stating that:

$$\begin{aligned} x &= Ax + y \\ L &= lx \end{aligned} \quad (16)$$

where A is the matrix of input coefficients, l the row vector of direct labor input coefficients, x the vector of total output, y the vector of final demand and L (scalar) total employment. Posing:

$$h = \frac{y}{L}, \quad M = \begin{pmatrix} A & h \\ l & 0 \end{pmatrix}, \quad \text{and} \quad q = \begin{pmatrix} x \\ L \end{pmatrix}$$

We obtain the following Equation:

$$Mq = q \quad (17)$$

it represents the economy's potential to self-reproduce if sectoral capacities are at level q . If $S_D = (c_i)_{1 \leq i \leq n+1}$ is the shock matrix, c_i being the fraction of production capacity of industry i destroyed by the disaster, the vector of remaining sectoral capacity can be expressed this way:

$$Remq = (I - S_D)q \quad (18)$$

meaning that if we consider that Equation (17) represents the pre-event situation of full employment and no idle capacity and that the matrix S_D is not null then:

$$M(I - S_D)q \neq S_Dq \quad (19)$$

unless $S_Dq = cq$ and in that case the economy is shrinking and only replicates at $100(1 - c)$ percent of its earlier level. In the other case, the same proportions cannot be replicated. In this case let us note t the changed total available inputs after the disaster then:¹³

$$M(I - S_D)q = t \quad (20)$$

Example 2: Post-disaster production optimization

Using data from example 1, we suppose the sectors can be decomposed into *Energy*, *Agriculture*, *Industries* and *Services* with the following input-output matrix:

Sector	A			
Energy	0.22	0.4	0.16	0.01
Agriculture	0.15	0.35	0.12	0.2
Industries	0.1	0.15	0.15	0.11
Services	0.45	0.1	0.25	0.1

¹³For more details, Steenge and Bočkarjova (2007) explain precisely the general case and the consequences.

Then, taking $l = \begin{pmatrix} 2.8 \\ 0.7 \\ 1.4 \\ 2.1 \end{pmatrix}$ as the vector of labor input coefficients meaning that in the energy sector, one unit of output needs the work of 2.8 people and in the agriculture sector, one unit of output needs the work of 0.7 people. Finally, we set $y = \begin{pmatrix} 60 \\ 25 \\ 12 \\ 42 \end{pmatrix}$ the vector of final demand (in Bn \$ US). Using Equations (16), we can respectively find the vector of total output: $x = \begin{pmatrix} 171 \\ 146 \\ 82 \\ 171 \end{pmatrix}$ and the total employment: $L = 1053$. Knowing that, we pose:

$$h = \frac{y}{L} = \begin{pmatrix} 0.057 \\ 0.024 \\ 0.011 \\ 0.040 \end{pmatrix}, \quad M = \begin{pmatrix} A & h \\ l & 0 \end{pmatrix} = \begin{pmatrix} 0.22 & 0.4 & 0.16 & 0.01 & 0.057 \\ 0.15 & 0.35 & 0.120 & 0.2 & 0.024 \\ 0.1 & 0.15 & 0.15 & 0.11 & 0.011 \\ 0.45 & 0.1 & 0.25 & 0.1 & 0.04 \\ 2.8 & 0.7 & 1.4 & 2.1 & 0 \end{pmatrix} \quad \text{and} \quad q = \begin{pmatrix} 171 \\ 146 \\ 82 \\ 171 \\ 1053 \end{pmatrix}$$

Doing so, we obtain a vector of demand ‘per capita’ h , an output vector extended to labor and we create a matrix M allowing us to link both Equations (16). We then can write the pre-disaster equilibrium both in terms of input-output and of labor, as Equation (17) states:

$$\begin{pmatrix} 0.22 & 0.4 & 0.16 & 0.01 & 0.057 \\ 0.15 & 0.35 & 0.120 & 0.2 & 0.024 \\ 0.1 & 0.15 & 0.15 & 0.11 & 0.011 \\ 0.45 & 0.1 & 0.25 & 0.1 & 0.04 \\ 2.8 & 0.7 & 1.4 & 2.1 & 0 \end{pmatrix} \begin{pmatrix} 171 \\ 146 \\ 82 \\ 171 \\ 1053 \end{pmatrix} = \begin{pmatrix} 171 \\ 146 \\ 82 \\ 171 \\ 1053 \end{pmatrix}$$

We suppose that the energy, agriculture, industries, services sectors and the employment experienced a loss of production capacity fraction after a natural disaster of 0.2, 0.3, 0.1, 0.1 and 0.15 meaning that:

$$I - S_D = \begin{pmatrix} 0.8 & 0 & 0 & 0 & 0 \\ 0 & 0.7 & 0 & 0 & 0 \\ 0 & 0 & 0.9 & 0 & 0 \\ 0 & 0 & 0 & 0.9 & 0 \\ 0 & 0 & 0 & 0 & 0.85 \end{pmatrix}$$

Equation (20) gives us:

$$\begin{pmatrix} 0.22 & 0.4 & 0.16 & 0.01 & 0.057 \\ 0.15 & 0.35 & 0.120 & 0.2 & 0.024 \\ 0.1 & 0.15 & 0.15 & 0.11 & 0.011 \\ 0.45 & 0.1 & 0.25 & 0.1 & 0.04 \\ 2.8 & 0.7 & 1.4 & 2.1 & 0 \end{pmatrix} \begin{pmatrix} 0.8 & 0 & 0 & 0 & 0 \\ 0 & 0.7 & 0 & 0 & 0 \\ 0 & 0 & 0.9 & 0 & 0 \\ 0 & 0 & 0 & 0.9 & 0 \\ 0 & 0 & 0 & 0 & 0.85 \end{pmatrix} \begin{pmatrix} 171 \\ 146 \\ 82 \\ 171 \\ 1053 \end{pmatrix} = \begin{pmatrix} 135 \\ 117 \\ 67 \\ 141 \\ 880 \end{pmatrix} \quad (21)$$

It shows that the economic equilibrium is perturbed because input and output-sides of the Equation (21) do not match. We can extract the 4 first rows of the equation corresponding to the input-output part without the influence of the sectoral interdependence equilibrium labor and we end up with the following:

$$\begin{pmatrix} 0.22 & 0.4 & 0.16 & 0.01 \\ 0.15 & 0.35 & 0.120 & 0.2 \\ 0.1 & 0.15 & 0.15 & 0.11 \\ 0.45 & 0.1 & 0.25 & 0.1 \end{pmatrix} \begin{pmatrix} 136.5 \\ 101.9 \\ 73.8 \\ 153.8 \end{pmatrix} + \begin{pmatrix} 51 \\ 21.3 \\ 10.2 \\ 35.7 \end{pmatrix} = \begin{pmatrix} 135 \\ 117 \\ 67 \\ 141 \end{pmatrix} \quad \text{as} \quad (I - S_D)q = \begin{pmatrix} 136 \\ 102 \\ 74 \\ 154 \\ 895 \end{pmatrix} \quad (22)$$

We need to raise an IO from the Equation (21) which will allow us to see what are the post-disaster possibilities *id est* we need to find an equation such as:

$$A\tilde{x} + \tilde{y} = \tilde{x} \quad \text{where} \quad \tilde{x} = \begin{pmatrix} 136 \\ 102 \\ 74 \\ 154 \end{pmatrix}$$

Hence, expected consumption in the post-disaster period is given by:

$$\begin{pmatrix} 0.22 & 0.4 & 0.16 & 0.01 \\ 0.15 & 0.35 & 0.120 & 0.2 \\ 0.1 & 0.15 & 0.15 & 0.11 \\ 0.45 & 0.1 & 0.25 & 0.1 \end{pmatrix} \begin{pmatrix} 136 \\ 102 \\ 74 \\ 154 \end{pmatrix} + \begin{pmatrix} 52.3 \\ 6.1 \\ 16.9 \\ 48.4 \end{pmatrix} = \begin{pmatrix} 136 \\ 102 \\ 74 \\ 154 \end{pmatrix} \quad (23)$$

Here, total demand y is adjusted. Equation (23) shows that the output from the energy sector drops to 136 after the disaster decreasing by 20% and the output from the agriculture sector drops to 101.9 decreasing by 30% compared to before the disaster. It also points out that the final demand of the energy is 52.3 and has suffered a 13% drop while the final demand of the agriculture is 6.1 and experienced a 76% drop.

Thus, using Equation (16), we can express \tilde{L} such that $\tilde{L} = l\tilde{x}$ corresponding to the equilibrium employment that the State is capable to ensure without loss:

$$\tilde{L} = (2.8 \ 0.7 \ 1.4 \ 2.1) \begin{pmatrix} 136.5 \\ 101.9 \\ 73.8 \\ 153.8 \end{pmatrix} = 880$$

We can compare this figure with the last component of $(I - S_D)q$ found in the Equation (22) which corresponds to the total employment available after the disaster and is equal to 895. We notice that the total employment available post-disaster is larger than the equilibrium employment meaning that the net output is not enough to satisfy the demand of the surviving workforce. There seems to be a disproportion between the losses in the economy and different sectors and the losses of workforce.

Lenzen *et al.* (2019) starts from Steenge and Bočkarjova (2007) method of determination of post-disaster possibilities but finds out that in some extreme cases it does not make sens. Indeed, let us bring back the example explained right above but supposing in this case that the sector 1 (Energy) has lost 80% of its production capacity. In this case:

$$I - S_D = \begin{pmatrix} 0.2 & 0 & 0 & 0 & 0 \\ 0 & 0.7 & 0 & 0 & 0 \\ 0 & 0 & 0.9 & 0 & 0 \\ 0 & 0 & 0 & 0.9 & 0 \\ 0 & 0 & 0 & 0 & 0.85 \end{pmatrix}$$

Equation (22) thus becomes:

$$\begin{pmatrix} 0.22 & 0.4 & 0.16 & 0.01 \\ 0.15 & 0.35 & 0.12 & 0.2 \\ 0.1 & 0.15 & 0.15 & 0.11 \\ 0.45 & 0.1 & 0.25 & 0.1 \end{pmatrix} \begin{pmatrix} 34 \\ 102 \\ 74 \\ 154 \end{pmatrix} + \begin{pmatrix} 51.2 \\ 21.3 \\ 10.2 \\ 35.7 \end{pmatrix} = \begin{pmatrix} 113 \\ 102 \\ 57 \\ 95 \end{pmatrix} \quad (24)$$

leading to this post-disaster I-O equation:

$$\begin{pmatrix} 0.22 & 0.4 & 0.16 & 0.01 \\ 0.15 & 0.35 & 0.12 & 0.2 \\ 0.1 & 0.15 & 0.15 & 0.11 \\ 0.45 & 0.1 & 0.25 & 0.1 \end{pmatrix} \begin{pmatrix} 34 \\ 102 \\ 74 \\ 154 \end{pmatrix} + \begin{pmatrix} -27.5 \\ 21.5 \\ 27.1 \\ 94.4 \end{pmatrix} = \begin{pmatrix} 34 \\ 102 \\ 74 \\ 154 \end{pmatrix} \quad (25)$$

meaning that we find a negative post-disaster final demand which economically does not make sens. We would want to find the maximum possible shock given an input-output matrix that economically makes sense using Cholesky decomposition. It would also be possible to correct an existing input-output matrix so that a reasonable shock could lead to accurate final demand values.

To guarantee the existence of a non-negative output vector that solves the equilibrium in the input-output model where final demand equals total output, the Hawkins-Simon condition for $(I-A)=B$ has to stand:

- (i) There exists an $x \geq 0$ such as $B \cdot x > 0$
- (ii) All the successive leading principal minors of B are positive, that is:

$$b_{11} \geq 0, \begin{bmatrix} b_{11} & b_{12} \\ b_{21} & b_{22} \end{bmatrix} > 0, \dots, \begin{bmatrix} b_{11} & b_{12} & \dots & b_{1n} \\ b_{21} & b_{22} & \dots & b_{2n} \\ \vdots & \vdots & \ddots & \vdots \\ b_{n1} & b_{n2} & \dots & b_{nn} \end{bmatrix} > 0 \quad (26)$$

The general method of Steenge and Bočkarjova (2007) is as follows: let x , y , A , L and l be respectively the production, final demand, input-output matrix, global employment and the vector describing the quantity of labor needed for one unit of output, all those before a disaster. Supposing that the country we consider undergoes an event destroying the fraction s_i of each industry i and e for the employment. We write:

$$S_D = \begin{pmatrix} s_1 & \dots & \dots & 0 \\ \dots & \ddots & \dots & \dots \\ \dots & \dots & s_{n-1} & 0 \\ \dots & \dots & 0 & s_n \end{pmatrix} \quad (27)$$

Therefore the post-disaster production and final demand are as follows:

$$\begin{cases} \tilde{x} = (I - S_D) \times x \\ \tilde{y} = (I - A) \times \tilde{x} \end{cases} \quad (28)$$

The difference with the cost-push Leontiev Input-Output method is that it addresses the issue of employment and we find that there is a difference between the equilibrium employment that the State is capable to ensure without loss after the extreme event being:

$$\tilde{L} = l\tilde{x} = \sum_{i=1}^n l_i(1 - s_i)x_i$$

and the total employment available after the disaster:

$$\hat{L} = (1 - e)L$$

Therefore, there can be a surge of unemployment after an extreme event because the workforce available is greater than what the state and the private actors are capable to economically ensure. Lenzen *et al.* (2019) chose a more comprehensive approach to tackle those issues that can be raised while looking for the most probable post-disaster consumption. They actually try to find non-negative post-disaster consumption that maximizes the sum of its coordinates while being solution of an Input-Output equation for which the output named x^1 will be actually smaller than the output \tilde{x} found in the Steenge and Bočkarjova (2007) method. They present the following mathematical input-output disaster analysis formulation: the level of total economic output x^0 of industry sectors $1, \dots, N$ after a disaster is given by:

$$\tilde{x} = (I - S_D) \cdot x \quad (29)$$

where S_D is a diagonal matrix with diagonal elements $s \in [0; 1]$ the direct consequences of the disaster and I identity matrix. The post-disaster consumption y^1 as the solution of the linear problem:

$$\max(\mathbf{1}y^1) \quad s.t. \quad \begin{cases} y^1 = (I - A)x^1 & \text{(i)} \\ x^1 \leq \tilde{x} & \text{(ii)} \\ y^1 \geq 0 & \text{(iii)} \end{cases} \quad (30)$$

where $\mathbf{1}$ is a line vector of ones and $A = Tx^{-1}$ is a matrix of input coefficients, while x^1 is the post disaster total economic input and T intermediate transaction matrix.¹⁴ A disaster implies a decrease in consumption levels: $y^1 = y - \Delta y$ which causes losses of value added and employment:

$$\Delta Q = q\Delta x = q(I - A)^{-1}\Delta y = \sum_{n=0}^{\infty} qA^n \Delta y \quad (31)$$

where q holds value added and employment coefficients.

Example 3: Post-disaster production optimization

As an example we are going to solve the Lenzen *et al.* (2019) optimization problem exposed earlier in this section. Continuing with previous example's data we are going to arbitrarily set the direct loss production matrix:

$$S_D = \begin{pmatrix} 0.2 & 0 & 0 & 0 & 0 \\ 0 & 0.3 & 0 & 0 & 0 \\ 0 & 0 & 0.1 & 0 & 0 \\ 0 & 0 & 0 & 0.1 & 0 \\ 0 & 0 & 0 & 0 & 0.15 \end{pmatrix}, \quad x = \begin{pmatrix} 171 \\ 146 \\ 82 \\ 171 \end{pmatrix} \quad \text{and} \quad A = \begin{pmatrix} 0.22 & 0.4 & 0.16 & 0.01 \\ 0.15 & 0.35 & 0.12 & 0.2 \\ 0.1 & 0.15 & 0.15 & 0.11 \\ 0.45 & 0.1 & 0.25 & 0.1 \end{pmatrix}$$

To find post-disaster consumption, we need to solve the following optimization problem (gathering Equations (25) and (30) together):

$$\begin{aligned} \max(\mathbf{1}y^1) \quad s.t. \quad & \begin{cases} y^1 = \begin{pmatrix} 0.78 & 0.6 & 0.84 & 0.99 \\ 0.85 & 0.65 & 0.88 & 0.8 \\ 0.9 & 0.85 & 0.85 & 0.89 \\ 0.55 & 0.9 & 0.75 & 0.9 \end{pmatrix} x^1 \\ x^1 \leq \begin{pmatrix} 136 \\ 102 \\ 74 \\ 154 \end{pmatrix} \\ y^1 \geq 0 \end{cases} \\ \iff \max(\mathbf{1}y^1) \quad s.t. \quad & \begin{cases} \begin{pmatrix} 0.51 & -2.751 & 5.348 & -3.403 \\ -2.434 & -0.9 & 2.108 & 1.392 \\ -2.575 & 8.712 & -7.57 & 2.573 \\ 4.268 & -4.679 & 0.931 & -0.346 \end{pmatrix} y^1 \leq \begin{pmatrix} 136 \\ 102 \\ 74 \\ 154 \end{pmatrix} \\ y^1 \geq 0 \end{cases} \end{aligned}$$

¹⁴The primary IO accounting relationship, designated as constraint (i) in Equation (30), implies that for every economy, the sum of intermediate demand, denoted as T , and the final demand, represented by y , is equal to the total output x . This is validated by the equation $y^1 = (I - A)x^1 = x^1 - T^1$, thus $T^1 + y^1 = x^1$. Constraint (ii) implies that in the immediate aftermath of a disaster, the total output cannot exceed the total output prior to the disaster minus the losses due to the disaster. Constraint (iii) mandates that the final demand, y , should always be greater than zero. This formulation, denoted as condition (i), deviates from the method employed in Steenge and Bočkarjova (2007), since it is essential in our case to confirm that the final demand, y , maintains a positive value (Lenzen *et al.*, 2019).

Using the *scipy.optimize* library in Python, we find the following post-disaster final demand: $y^1 \approx \begin{pmatrix} 0 \\ 21.49 \\ 27.11 \\ 94.44 \end{pmatrix}$ and the post-disaster output: $x^1 \approx \begin{pmatrix} 85.27 \\ 126.31 \\ 88.30 \\ 186.13 \end{pmatrix}$. In this case, we observe that the final demand of the first sector drops from 60 to 0, meaning that the first sector has no more demand while the second sector's demand is relatively stable from 21.3 to 21.49. The production of every sectors are widely negatively impacted: first sector knows a huge drop of about 50% of its production (from 171 to 85.27) while the second a moderate of about 13.5%. The fact that the first sector is on all sides more affected than the second one is obviously to be linked to the fact that the first sector is shocked up to 80% while the second one of *only* 30% which is almost equal to the loss of production in both cases.

Remark 2 Equations 28 present a linear relationship between total output, final demand, total employment and the direct losses of each sector. It allows to have an understandable and practicable representation, not too sensitive to improper modeling. However, in practice, the relationships between each of these variables might not be linear, as introduced in the previous paragraph and from Sandberg (1973). From 18, we can adapt the equations of Hallegatte (2008) to our extreme events representation, taking into account indirect shocks to the economy. It is to be noted that the calibration of pass-through rates has to be adapted to post-disaster production and final demand equilibrium.

$$\begin{aligned} \tilde{x} &= \left(I - S_{DI} \cdot \left[1 + \phi \times (I_n - A^\top)^{-1} \right] \right) \times x \\ \tilde{y} &= (I - A) \times \tilde{x} \end{aligned} \tag{32}$$

3.3 Adaptive regional input-output (ARIO) model

Hallegatte (2008) introduces a framework accounting for input-output adaptation including a temporal response. This model allows us to compute the output, demand, price and adapted matrix of technical coefficients after a shock. It also introduces a temporal dimension, and depicts the return to equilibrium of both coefficients and sectoral activities after the event (i.e. original value of input-output matrix and output). The framework is illustrated with the tropical cyclone Katrina (2005).

3.3.1 Seminal adaptive framework (Hallegatte, 2008)

Let $x_{max,i}^t$ be the maximum output vector of sector i , at time t . It represents the maximum production this sector including potential overproduction capacities (e.g. construction sector). The process is illustrated in Figure 4 and Figure 14. For each time t , we follow next steps to compute the output and final demand.

1. At $t = 0$, we initialize our vectors and matrix all equal to the vectors pre-disaster ($A^{t_0} = A_b, \dots$). The shocked final demand becomes :

$$y_i^{t_0} = y_i^b + D_i$$

denoting the final demand pre-disaster including additional reconstruction demand D implied by the events.

2. We compute a first-guess output vector:

$$x_0^t = (I - A)^{-1} y = y_0^t$$

3. Then, we address the production capacity of each industry, the production of each sector cannot exceed its own production capacity $x_{\max,i}^t$. Thus:

$$x_{1,i}^t = \min\{x_{\max,i}^t, y_{0,i}^t\} \quad (33)$$

4. For each given industry i , we establish the volume of orders that it is mandated to satisfy on behalf of other industries:

$$O_{1,i}^t = \sum_j A_{i,j}^t x_{1,j}^t$$

Either industry i possesses the capacity to adequately supply its commodities to all other industries, thereby not exerting any influence on the operations of these industries, or industry i is incapable of fulfilling the demand for its commodities, consequently imposing restrictions on the entirety of the other dependent industries. It leads to the computation of a new output vector:

$$x_{2,i}^t = \min\{x_{1,i}^t, \text{for all } j: \frac{x_{1,j}^t}{O_{1,j}^t} x_{1,i}^t\} \quad (34)$$

5. We therefore have two options:

- if $x_1^t = x_2^t$, there is no bottleneck and we can compute all our variables at time t :

$$x^t = x_2^t, \quad y^t = (I - A)x^t, \quad \text{for all industry } i: \quad p_i^t = p_i^b \left(1 + \gamma_p \frac{y_i^t - x_i^t}{x_i^t}\right) \quad (35)$$

- if $x_1^t \neq x_2^t$, there is a consistency problem ; we do not consider that each industry that produces less will also ask for less to its suppliers. We then compute a new total demand y_1^t satisfying:

$$y_{1,i}^t = y_i^t + \sum_j A_{i,j}^t x_{2,j}^t \quad (36)$$

6. we replace this value of total demand in the Equation (33) until we have convergence of the value of total output (a decreasing sequence lower-bounded by 0 is guaranteed).

Time dependence and return to normal For each industry j , the update of time-depending variables follows:

- If $x_j^t < y_j^t$, the industry cannot produce enough to satisfy demand, then:

$$\begin{aligned}
 \alpha_j^{t+1} &= \alpha_j^t + (\alpha_{\max,j} - \alpha_j^t) \frac{y_j^t - x_j^t}{y_j^t} \frac{\Delta t}{\tau} \\
 A_{i,j}^{t+1} &= A_{i,j}^t - A_{i,j}^t \frac{y_j^t - x_j^t}{y_j^t} \frac{\Delta t}{\tau} \text{ if } i \in I_{local} \text{ and } j \in J_{local} \\
 A_{i,j}^{t+1} &= A_{i,j}^t - A_{i,j}^t \frac{y_j^t - x_j^t}{y_j^t} \frac{\Delta t}{\tau} \text{ if } i \in I_{local} \text{ and } j \notin J_{local} \text{ (exports)} \\
 A_{i,j}^{t+1} &= A_{i,j}^t + A_{i,j}^t \frac{y_j^t - x_j^t}{y_j^t} \frac{\Delta t}{\tau} \text{ if } i \notin I_{local} \text{ and } j \in J_{local} \text{ (imports)} \\
 A_{i,j}^{t+1} &= A_{i,j}^t \text{ if } i \notin I_{local} \text{ and } j \notin J_{local}
 \end{aligned} \tag{37}$$

where $\alpha_{\max,j}$ is the maximum capacity to overproduce and $\alpha_{t,j}$ designs the level of overproduction at t .

- If $x_j^t > y_j^t$, the industry is capable to meet the demand. The production will return to normal (as before the disaster) and then:

$$\begin{aligned}
 \alpha_i^{t+1} &= \alpha_i^t + (\alpha_i^b - \alpha_i^t) \frac{\Delta t}{\tau} \\
 A_{j,i}^{t+1} &= A_{j,i}^t + \left(\epsilon + \frac{A_{j,i}^t}{A_{j,i}^b} \right) (A_{j,i}^b - A_{j,i}^t) \frac{\Delta t}{\tau} \text{ if } i \in I_{local} \text{ and } j \in J_{local} \\
 A_{j,i}^{t+1} &= A_{j,i}^t + \left(\epsilon + \frac{A_{j,i}^t}{A_{j,i}^b} \right) (A_{j,i}^b - A_{j,i}^t) \frac{\Delta t}{\tau} \text{ if } i \in I_{local} \text{ and } j \notin J_{local} \text{ (exports)} \\
 A_{j,i}^{t+1} &= A_{j,i}^t - \left(\epsilon + \frac{A_{j,i}^t}{A_{j,i}^b} \right) (A_{j,i}^b - A_{j,i}^t) \frac{\Delta t}{\tau} \text{ if } i \notin I_{local} \text{ and } j \in J_{local} \text{ (imports)} \\
 A_{i,j}^{t+1} &= A_{i,j}^t \text{ if } i \notin I_{local} \text{ and } j \notin J_{local}
 \end{aligned} \tag{38}$$

With our new variables we can also update the production capacity (with v_i the value added of the industry i):

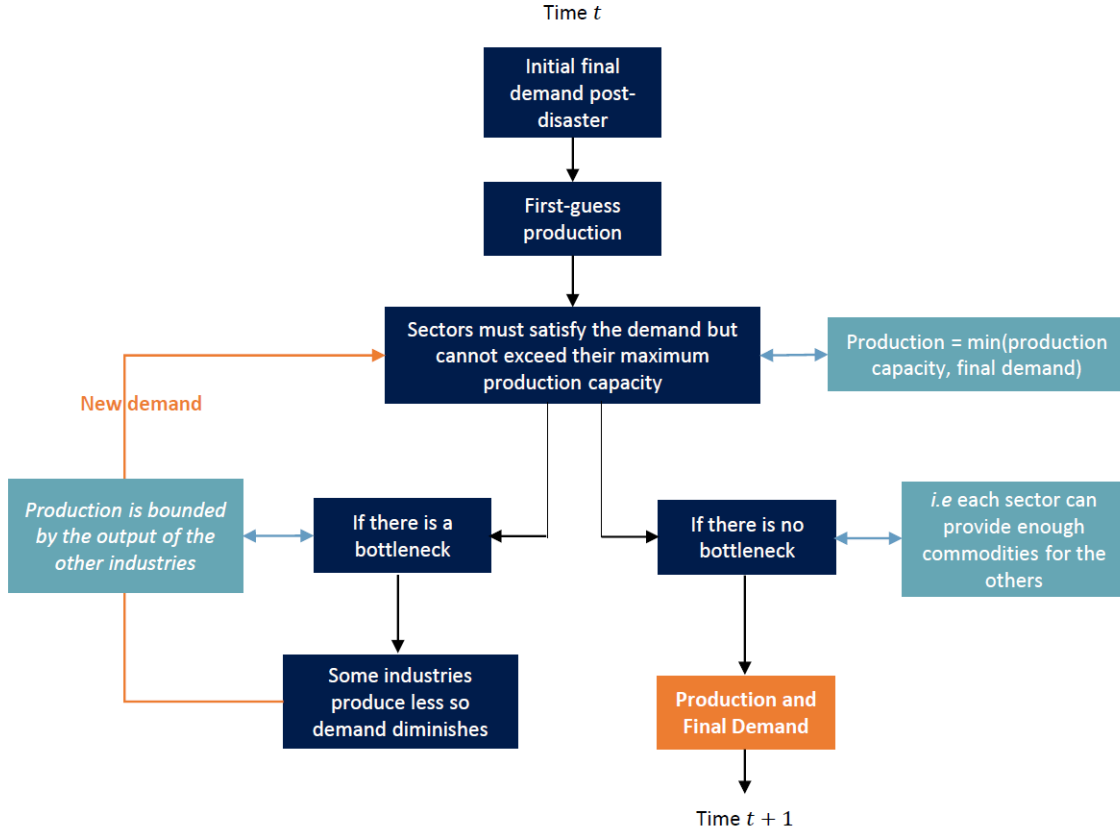
$$x_{\max,i}^t = x_i^t \left(1 - \frac{D_i}{4v_i} \right) \alpha_i^t$$

Subsequently, we can now compute our variables at time $t + 1$ and so on for all the time we want to study the consequences of our disaster.

Figure (4) (and Figure (14) in annex for further explanations) present the breakdown of the steps of Hallegatte (2008) method of finding the post-disaster consumption at time $t + 1$. Starting from the value of production at time t , we first calculate the first-guess production required. Then, including maximum production capacity x_{\max}^t at time t (which acts as the upper boundary), we may fix the value of $x_{1,i}^t$. From here, there are two possibilities, either

(i) the production value is greater than the amount of orders that the industry is required to fulfill by other industries thus there is no other industries impacted, or (ii) the production is strictly smaller and then every other industry experiences a limitation.

Figure 4: Breakdown of the steps of Hallegatte (2008) at each time t



Finally, if the computed production is equal to the one before, we can say that there is no bottleneck and that we actually have found the true production value. In the other case, we take into consideration the change of total demand of the industries due to the reduction of production. Then, we re-inject this value of total demand to the step where we take into account the production capacity. A loop is established and we follow it up to $x_{k-1} = x_k$ eventually happens and equilibrium production is found (see above for equations and explanations of the different variables and a simple example). Thus, we set the value of output at time $t + 1$ as $x_k = x^{t+1}$ and the total demand is $y^{t+1} = (I - A)^{-1}x^{t+1}$. From there we update the values of α and of the matrix input-output A as it is explained in Equations (37) or (38) depending on the situation.

Example 4: Adaptive regional input-output model

Let us introduce the vector of total final demand, the Input-Output matrix and the production capacity vector^a:

$$y = \begin{pmatrix} 60 \\ 25 \\ 12 \\ 42 \end{pmatrix}, \quad A = \begin{pmatrix} 0.55 & 0.15 & 0.16 & 0.01 \\ 0.15 & 0.35 & 0.12 & 0.2 \\ 0.08 & 0.05 & 0.62 & 0.01 \\ 0.05 & 0.1 & 0.05 & 0.56 \end{pmatrix} \quad \text{and} \quad x^{max} = \begin{pmatrix} 250 \\ 180 \\ 125 \\ 200 \end{pmatrix}$$

The first-guess production is calculated as follows:

$$x^0 = (I - A)^{-1}y = \begin{pmatrix} 229 \\ 163 \\ 106 \\ 171 \end{pmatrix} = y^0 \quad (39)$$

Since $x_i^1 = \min\{x_i^{max}, y_i^0\}$, we therefore have: $x_i^1 = y_i^0$. Then, we have the first-guess amount of orders that the industry i requires being: $O_i^1 = \sum_j A_{i,j}x_j^1$, as a result we have:

$$O^1 = \begin{pmatrix} 141 \\ 350 \\ 563 \\ 100 \end{pmatrix}$$

Therefore

$$\begin{cases} x^1(1) \geq O^1(1) \\ x^1(2) < O^1(2) \\ x^1(3) < O^1(3) \\ x^1(4) \geq O^1(4) \end{cases} \iff \begin{cases} x^2(1) = \min\{x^1(1), \forall j \frac{x^1(j)}{O^1(j)}x^1(1)\} \\ x^2(2) = x^1(2) \\ x^2(3) = x^1(3) \\ x^2(4) = \min\{x^1(4), \forall j \frac{x^1(j)}{O^1(j)}x^1(4)\} \end{cases} \iff x^2 = \begin{pmatrix} 43 \\ 163 \\ 106 \\ 32 \end{pmatrix} \quad (40)$$

Hence the production $x^1 \neq x^2$ so we have to adapt the total final demand to the

decrease of the production according to Equation (36): $y^1 = \begin{pmatrix} 97 \\ 159 \\ 92 \\ 66 \end{pmatrix}$. From there, we

re-inject the value of y^1 into the Equation (33) which gives $x^3 = y^3$. This leads us to a new amount of order that each industry has to satisfy:

$$O^2 = \begin{pmatrix} 96 \\ 181 \\ 239 \\ 62 \end{pmatrix}$$

In the same way than Equation (40) we have:

$$x^4 = x^3$$

we are able to find convergence of the value of production (and *a fortiori* convergence of the total final demand), being in this example:

$$x^\infty = \begin{pmatrix} 97 \\ 159 \\ 92 \\ 66 \end{pmatrix} \quad \text{and} \quad y^\infty = y^3 = \begin{pmatrix} 145 \\ 155 \\ 82 \\ 92 \end{pmatrix}$$

We see an increase of the final demand of every sector, indeed the final demand of sector 1 goes from 60 to 145 hence an increase of 141% and the one from from sector 2 from 25 to 155 thus an increase of more than 500%. The production is also strongly affected by the disaster. The first sector's production is decreased from 229 to 97 (57% is lost), while the second sector's production stays relatively even from 163 to 159 partly thanks to its capacity to overproduce.

^athe value of the production is here arbitrary but Hallegatte (2008) gives a method to calculate it according to the damages vector, the annual value-added and the capacity to overproduce of the sectors)

Remark 3 *Hallegatte (2008) introduces a thorough approach, primarily focusing on the ability to observe and calculate the progression of key economic indicators over time following a severe event. However, this process is quite complex, and many crucial endogenous variables are either overly specific to the case of the Katrina Tropical Cyclone (2005) in Louisiana, or are not explicitly included in the method. These missing variables include initial or peak overproduction capacities, the temporal characteristics of variable increase and decrease, and the additional demand placed on sectors due to the direct shock. We cannot arbitrarily assign values to these variables as it would significantly influence the results of our method, leading to inconsistent and unreliable predictions.*

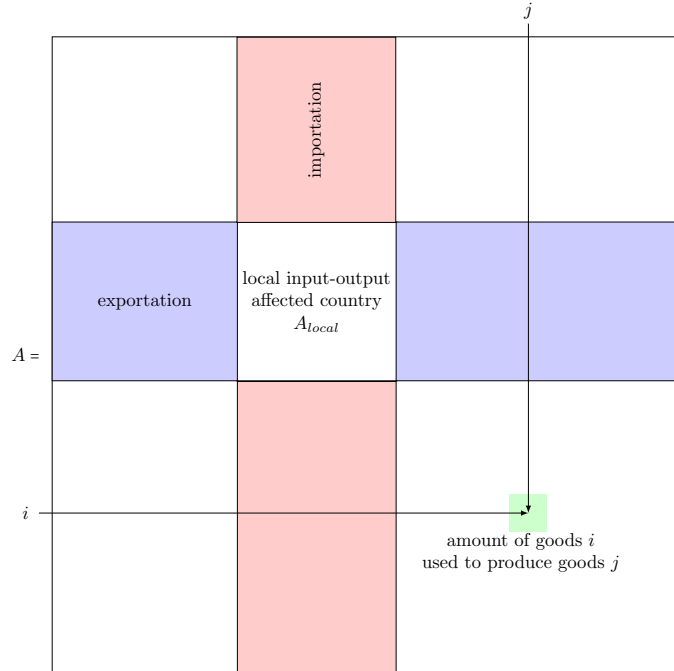
3.3.2 Implementing the ARIO approach (BoARIO, Hallegatte, 2013)

There has been significant improvement since (Hallegatte, 2008) seminal work. For instance, the package BoARIO¹⁵ is a python implementation project of the Adaptive Regional Input Output (ARIO) model described in Hallegatte (2013) with improvement from Guan *et al.* (2020) including world input-output matrices available in pymrio from (Stadler, 2021). Thus, internal exchanges and the aggregate imports / exports variable of the seminal Hallegatte (2008) approach can be adapted to world input output tables (c.f. Table 5).

In simple terms, the model explains how shocks, or sudden changes, spread through the economy day by day. When there is a mismatch between how much product is being made by a given industry and how much intermediate and final demand are being required, the model adapts the outputs. This might mean that some businesses may not get everything they optimally require. Households also deal with not getting what they wanted in this

¹⁵Available at: <https://spjuhel.github.io/BoARIO>.

Figure 5: From local to multi-regional input-output



representation without asking for it at a later stage. Businesses can use their stored supplies to make up for what they did not get and might ask for more at the next time step. Rebuilding sectors also have a limited latitude to increase their production and match rebuilding demand to a greater extent. At each time step, businesses adapt how much they produce and order based on what they need and what they have in stock.

The direct economic impact represents how much the initial shock affects the economy. The total economic impact also includes the knock-on effects as the shock spreads out. We can look at the total impact in two ways: (i) Unmet demand: when households can no longer buy what they need because of the shock and (ii) Change in production: when businesses build more or less products than what they did before the shock. In the following, the economy is modeled as a set of economic sectors and a set of regions. An industry is a specific (sector, region) couple. Each economic sector has to produce and draws inputs from an inventory and from other sectors. The total demand consists of a final demand (household consumption, public spending and private investments) coming from all the connected regions (i.e. both local demand and exports), an intermediate demand (inventory resupply) and a rebuilding demand (where each affected sector/region asks for products from itself and other rebuilding sectors). An initial equilibrium state of the economy is built based on MRIO tables.

The process initial state is as follow:¹⁶

$$\begin{cases} x_0 &= Z \cdot i + Y \cdot i \\ A &= Z \cdot \hat{x}_0^{-1} \\ A_{va} &= Z \cdot \hat{x}_0^{-1} \end{cases}$$

Technology and transactions information is required at sector level, regardless of the region of provenance. We compute the following¹⁷:

$$Z^{Share} = Z \oslash \left(Z^S \otimes \underbrace{\begin{bmatrix} 1 \\ \vdots \\ 1 \end{bmatrix}}_{m\text{-sized}} \right) \quad (41)$$

$Z^S = I_{sum} \cdot Z$

¹⁸ Then the initial inventories matrix is:¹⁹

$$\Omega(t_0) = \underbrace{[s \dots s]}_{n \text{ times}} \oslash \begin{bmatrix} x(0) \\ \vdots \\ x(0) \end{bmatrix} \oslash A^S = \begin{bmatrix} s_1 x_1(0) a_{11} \dots s_1 x_p(0) a_{1p} \\ \vdots \\ s_n x_1(0) a_{n1} \dots s_n x_p(0) a_{np} \end{bmatrix} \quad (42)$$

where $w_{pi}(0) = s_p \cdot x_i(0) \cdot a_{pi}$ is the exact amount of product p required by industry i to produce $x_i(0)$ (i.e. initial equilibrium production of i) during s_i temporal unit, or, alternatively, that i could (technically) produce during s_t temporal units without receiving input from any industry producing p .

The order matrix $O = Z$ at the initial state. Then, production is driven by demand, (each sector cannot produce more than demand), while being constrained by the orders to required industries. Introducing the vector of overproduction capacity $\alpha = (\alpha_i)$ and $\Delta_i(t)$ the initial or 'direct shock' of production capacity of an industry i , the vector of equilibrium production capacity becomes at each time step:

$$x_i^{cap} = \alpha_i(t)(1 - \Delta_i(t))x_i(t) \quad (43)$$

¹⁶In this section, we present the functioning of the module available at <https://spjuhel.github.io/BoARIO/BoARIO-math.html>.

¹⁷ I is a row summation matrix of concatenated identity matrices of size $r * s$

¹⁸ \oslash is the Kronecker product which repeats each row of Z^S m times.

\otimes is the matrix element-wise division (including that if initial order to an industry was null, the share ordered is also null).

¹⁹ A^S and Z^S are aggregated technology and transition at the sector level.

the realized actual production at each time follows:

$$\left\{ \begin{array}{l} D^{Tot}(t) = O(t) \cdot \begin{bmatrix} 1 \\ \vdots \\ 1 \end{bmatrix} + Y \cdot \begin{bmatrix} 1 \\ \vdots \\ 1 \end{bmatrix} + \Gamma \times \tau_{REBUILD} \\ x^{Opt}(t) = (\min(d_i^{Tot}, x_i^{Cap})) \\ \Omega^{Cons}(t) = \begin{bmatrix} s_1^1 & \dots & s_1^p \\ \vdots & \ddots & \vdots \\ s_n^1 & \dots & s_n^p \end{bmatrix} \odot \begin{bmatrix} x^{Opt}(t) \\ \vdots \\ x^{Opt}(t) \end{bmatrix} \odot A^S \cdot \psi \\ x^a(t) = \begin{cases} x_i^{Opt}(t) & \text{if } w_p^i(t) > w_p^{Cons,i}(t) \forall p \\ x_i^{Opt}(t) \cdot \min_{p \in S} \left(\frac{w_p^s(t)}{w_p^{Cons,i}(t)} \right) & \text{if } w_p^i(t) < w_p^{Cons,i}(t) \forall p \end{cases} \end{array} \right.$$

where each equation represents respectively:

- Total demand D^{Tot}
- Optimal production without inventory constraints for each industry x^{Opt}
- Inventory constraint for each input $\Omega^{Cons}(t)$, as the share ψ of the quantity of stock required to produce s_p^i temporal unit of production at the level of previous step.

Then, distribution module defines how actual production is allocated towards demands from other sectors. The following equation materializes that each client will receive a share of their order as a proportional rationing scheme if the demand of industry i is greater than its production.

$$\left\{ \begin{array}{l} O^{Received}(t) = \left(\frac{o_{ij}(t)}{d_i^{Tot}(t)} \cdot x_i^a(t) \right)_{i,j} \\ Y^{received} = \left(\frac{y_i}{d_i^{Tot}(t)} \cdot x_i^a(t) \right)_i \\ \Gamma^{Repair}(t) = \left(\frac{\gamma_i \cdot \tau_{REBUILD}}{d_i^{Tot}(t)} \cdot x_i^a(t) \right)_i \end{array} \right.$$

Remark 4 *logically, if the inventory of product $p \in S$ of an industry i is lower than its required level then i 's production is reduced ; an inventory reduction of $x\%$ leads to $x\%$ reduction in production, everything else being equal.*

where γ_i is the total rebuilding demand towards industry i and $\tau_{REBUILD}$ is the rebuild characteristics time²⁰. The inventory resupply can be modeled using the received orders, the model describes the change in inventories through time with:

$$\Omega(t+1) = \Omega(t) + \underbrace{\left(I_{sum} \cdot O^{Received}(t) \right)}_{\text{orders aggregated by inputs}} - \underbrace{\left(\begin{bmatrix} x^a(t) \\ \vdots \\ x^a(t) \end{bmatrix} \odot A^S \right)}_{\text{input used during production}} \quad (44)$$

²⁰see notation section in appendix.

During the recovery period we have:

$$\Gamma_{Tot}(t+1) = \Gamma_{Tot}(t) - \Gamma^{Repaired}(t) \quad (45)$$

After distribution, the model computes the orders made by each industry towards others to resupply their inventories of inputs. They seek to restore their inventories to their initial level with regards to the current equilibrium production level.

$$\begin{aligned} \Omega^*(t) &= s_p^i \cdot \begin{bmatrix} x^{Opt}(t) \\ \vdots \\ x^{Opt}(t) \end{bmatrix} \odot A^S \quad \text{Inventory goals} \\ \Omega^{Gap}(t) &= (\Omega^*(t) - \Omega(t))_{\geq 0} \quad \text{Inventory gaps} \\ O^S(t) &= \frac{1}{\Gamma_{Inv}} \cdot \Omega^{Gap}(t) + \begin{bmatrix} x^a(t) \\ \vdots \\ x^a(t) \end{bmatrix} \odot A^S \quad \text{Intermediate demand total orders} \\ O(t) &= \left(O^S(t) \otimes \underbrace{\begin{bmatrix} 1 \\ \vdots \\ 1 \end{bmatrix}}_{m\text{-sized}} \right) \odot Z^* \quad \text{Intermediate demand orders} \end{aligned} \quad (46)$$

In Inventory goals, we compute orders based on optimal production. In Inventory gaps $(A-B)_{\geq 0}$ is used. In Intermediate total demand orders, total orders for intermediate demand are being aggregated. Finally, in Intermediate demand orders, the actual order matrix is being calculated.

The model has two variants based on the value of Z^* which drive possible substitution between suppliers:

- A. Initial transaction shares are used: $Z^*(t) = Z^{Share}$ and in this case there is no possible substitution among suppliers.
- B. The model uses initial transaction share, but now weighted by suppliers current production level relative to their initial production. Both occurrences of Z in (37) now follow:

$$Z \odot \begin{bmatrix} \frac{x_1(t)}{x_1(0)} & \cdots & \frac{x_p(t)}{x_p(0)} \\ \vdots & \ddots & \vdots \\ \frac{x_1(t)}{x_1(0)} & \cdots & \frac{x_p(t)}{x_p(0)} \end{bmatrix} \quad (47)$$

In ARIO, industries also have the possibility to temporarily increase their production capacity as defined previously via an overproduction mechanism. BoARIO uses a scarcity index:

$$\zeta(t) = \frac{d_i^{Tot}(t) - x_i^a(t)}{d_i^{Tot}(t)}$$

$$\alpha_i(t+1) = \begin{cases} \alpha_i(t) + (\alpha^{max} - \alpha_i(t)) \cdot \zeta(t) \cdot \frac{1}{\Gamma_\alpha} & \text{if } \zeta(t) > 0 \\ \alpha_i(t) + (\alpha^b - \alpha_i(t)) \cdot \frac{1}{\Gamma_\alpha} & \text{if } \zeta(t) \leq 0 \end{cases} \quad (48)$$

Currently, the model allows representing the impact of an event via three effects:

1. A decrease of the production capacity of the impacted industries (destruction of productive capital)
2. An additional final demand towards rebuilding sectors.
3. An arbitrary reduction of the production capacity for a given period.

The production capacity decrease is modeled assuming that an event happens at $t = E$, causing Γ_{Tot} damages to the different industries. Defining $\Delta_i(t = E)$ the initial (when an event occurs) loss of production capacity of industry i , as the fraction of capital destroyed over its capital stock:

$$\Delta_i(t = E) = \frac{\gamma_i(t = E)}{k_i} \quad (49)$$

We update Δ_i during every step with remaining damage:

$$\Delta_i(t) = \frac{\gamma_i(t)}{k_i} \quad (50)$$

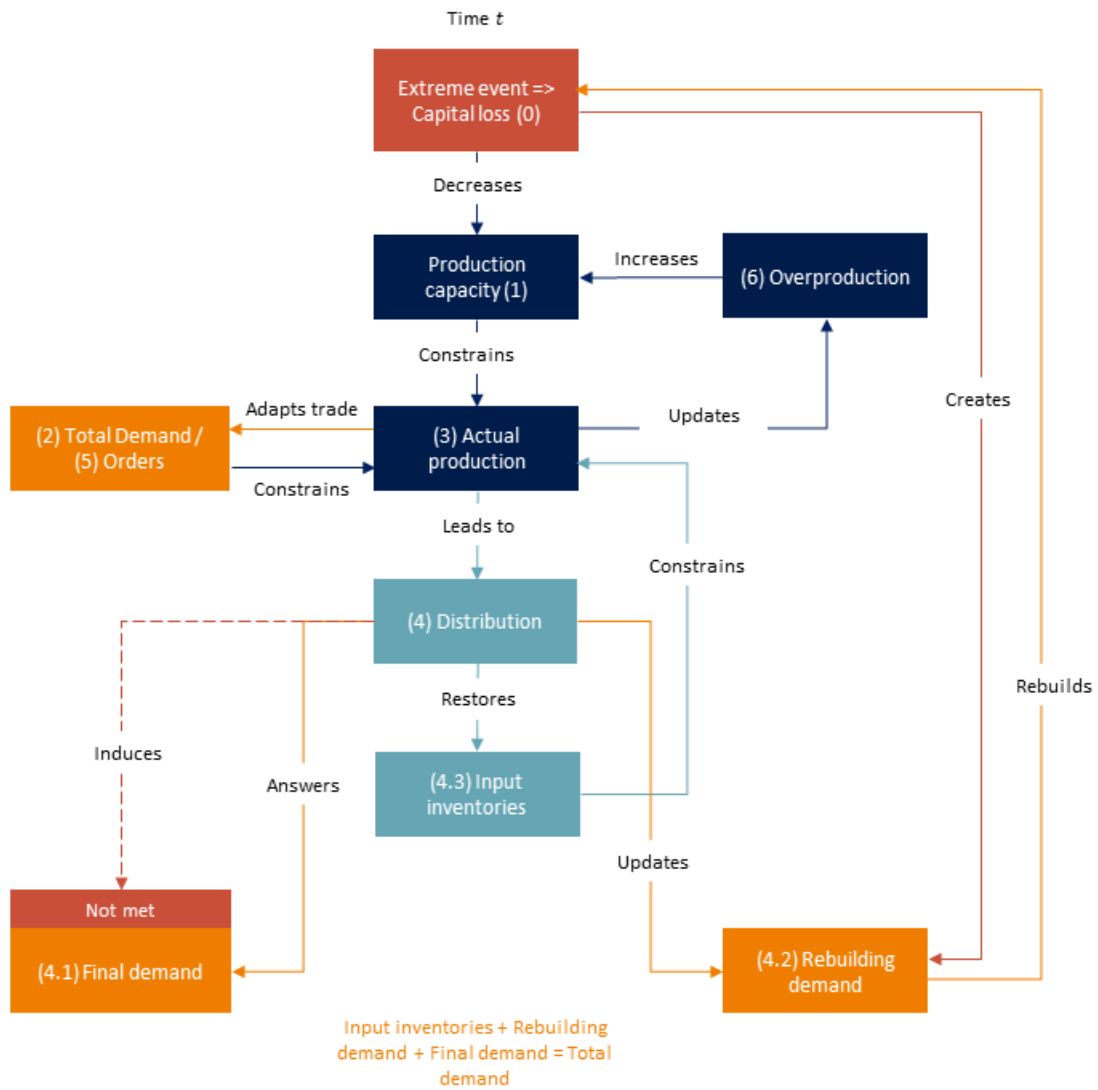
Figure 6 provides a systemic representation of the response of a production-distribution model to an exogenous shock that induces capital loss in the form of a flow graph. The initial perturbation results in a reduction of the system's production capacity. This change then propagates through the system, leading to a deviation from expected production outputs.

A disruptive event occurs (0), then the production-distribution system experiences capital loss, causing a decrease of production capacity labeled as (1). This decrease subsequently constrains the actual production output (3). As time passes, the distribution (4) endeavors to replenish input inventories, thereby stabilizing the system in the wake of the shock.

Total demand and orders (2), are being continually adapted to account for the prevailing trade constraints. This adaptation is influenced by the reduced actual production and the system's attempt to re-calibrate itself within the new constraints imposed by the capital loss. The discrepancy between the supply capabilities and market demand gives rise to a notional final demand (4.1), which is under continuous review as the system seeks equilibrium.

Concurrently, a feedback loop stemming from overproduction (6), leads to an increase in production capacity. This paradoxical response may create a surplus, further complicating the system's return to a balanced state. The feedback and adaptive processes in the system are critical for managing orders (5) and demand in the face of unexpected disruptions, as they attempt to reach a simplified state of the economy that matches reality.

Figure 6: Breakdown of the steps of (Hallegatte, 2013) from disaster to final production and demands



3.4 Comparison of diffusion approaches

We compare in this paper several methods of diffusion of physical risks to estimate the indirect costs of extreme events using the example of tropical cyclones and we propose with a Monte-Carlo simulation an approximate forecast of the surge of costs of extreme events from now to 2100. To do so, we use a Multi Regional Input-Output model working with the Exiobase3 database. The characteristics of each method we have used is compiled in Table 4.

Table 4: Characteristics of each method

	Cost-push	Optimization	Adaptive
Time dependency	-	-	+
Optimization	-	+	+
Labor account	-	+	-
Generalizable	++	+	-
Time efficiency	+	-	-

The cost-push method is the simplest method of the three. Even though the Optimization method allows us to take into account the labor, it is computationally more demanding. As for the Adaptive method, it brings the interesting time dependency but it has originally been built on the specific case of the Katrina cyclone occurring in the US in 2005 and a lot of parameters need a very precise calibration with a real challenge to generalize properly to every event.

The BoARIO method presents a nuanced approach to assessing the temporal impacts of a specific event on a production-distribution system. This approach is commendable for its ability to detail the sequential repercussions of capital loss on production capacity, actual output, and the subsequent demand response. It captures the intricate dynamics of the system’s adaptive behavior and feedback mechanisms in real-time, thus providing a granular understanding of the event’s immediate and downstream effects.

However, when integrating this model within a Monte Carlo framework (c.f. section 4) for the evaluation of annual risks, one must consider the method’s alignment with the probabilistic nature of such simulations. In the context of annual basis assessment, the model’s intricate real-time responses are likely to be averaged out or ‘smoothed’ over time, diluting the granularity of the temporal response.

Given this temporal smoothing effect, a simplified model that focuses on the cost-push cascading effects may indeed prove more efficient for the purposes of a Monte Carlo assessment. This streamlined approach would emphasize the propagation of indirect costs resulting from physical risks, capturing the broader financial implications without the detailed temporal resolution unnecessary for long-term risk assessments. Such a model, though less detailed in the immediate aftermath of a risk event, would effectively quantify the cumulative financial impact over the annual period, which aligns with the objectives of a Monte Carlo risk analysis. It allows for a computationally less intensive and more strategically focused estimation of risk exposure, providing a macroeconomic perspective on potential financial vulnerabilities induced by physical risk events.

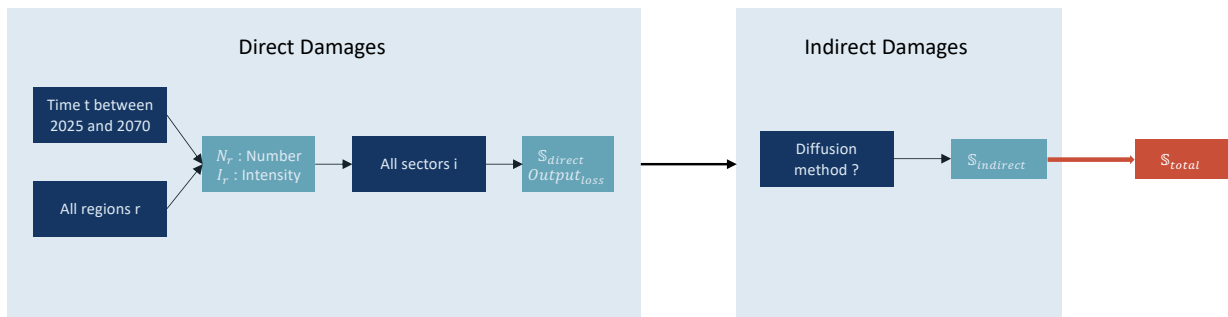
4 Physical Value-at-Risk and Empirical Applications

In this section, we show how to introduce physical risk in the transition risk framework defined in Desnos *et al.* (2023), adapting it for the physical risks case. For simplicity, and because of the considerations listed in Section 3.4, we use a classic Leontief diffusion in the model. We also illustrate some case studies of the implementation of the Boario framework, particularly relevant for specific event analysis. As a reminder, current paper focuses on tropical cyclones example and gives hints as to how to generalize the methodology to other climate change related extreme events.

4.1 Monte Carlo algorithm for direct damages

Based on the subsection (2.2), we can implement a Monte-Carlo algorithm to calculate a sample of direct damages due to tropical cyclones between 2025 and 2070.

Figure 7: Method for the simulation of direct damages



The damages are calculated as described in the Section 2.2. We introduce historical frequency and intensity from historical data and an illustrative climate induced increase of the damage (e.g. representing extreme event frequency and severity) of 4%.

However, we know that different sectors of a country which undergoes an extreme event may not suffer the same consequences. Indeed, sectors which rely highly on physical assets (Construction, Agriculture, Mining...) will be more affected than sectors that do not (Lenzen *et al.*, 2019). For this reason, we suppose that sectors that do not rely on physical assets will not suffer any direct damages and that all of the losses revolve around the physical assets relying sectors, except for the insurance sector. Furthermore, for a single extreme event, the losses of the different sectors cannot be independent so we add a correlation of 80% between the variables describing the losses of each sector for a single event. In these illustrative simulations, a country cannot lose more than its GDP.

Algorithm 1 Monte Carlo algorithm for direct damages

λ_r feature of number of cyclone per region

Inputs σ_r global standard deviation of damages
 μ_r global mean of damages N number of simulations

for N **do**
 for t between 2025 and 2070 **do**
 for all region r **do**
 $N_r \leftarrow \mathcal{P}(\lambda_r)$ \triangleright the number of extreme events in the region
 for all sector relying on physical assets i **do**

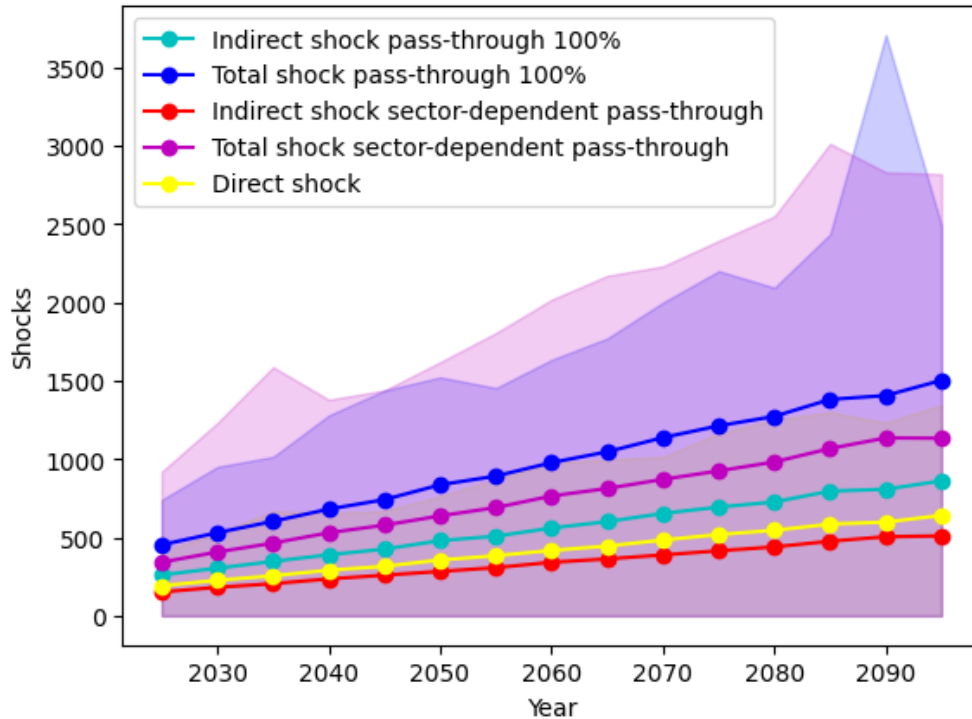
$$\xi_{i,r} \leftarrow N_r \times \log \mathcal{N}(\mu_r, \sigma_r) \times (0.04t - 79.8)$$

$$\times (\mathbb{1}_{t \in]0;1a]} 0.3 + \mathbb{1}_{(t=0) \cup (t > 1a)})$$
 \triangleright fraction loss of this sector
 end for
 for all sector not relying on physical assets i **do**
 $\xi_{i,r} \leftarrow 0$ \triangleright No losses
 end for
 end for
 $\mathbb{S}_{\text{direct}} \leftarrow \text{diag}(\xi_{i,r})$
 Output loss = $\mathbb{S}_{\text{direct}} \times x$
 end for
 end for

4.2 Results and Operational Implication

Physical Value-at-Risk Combining the Monte Carlo algorithm for direct damages and the input-output diffusion, we are able to achieve initial outcomes. We explore 2 pass-through settings, with 5 000 simulations and compute the indirect losses for both cases. The first one supposes that all the losses are passed onto prices meaning that we put a pass-through being equal to 100% for all the sectors (teal and blue dots in Figure 8). The second is the implementation of the pass-through described in the paragraph 3.1, with a penalty of 0.428 calibrated using indirect losses from regional cyclones from the literature. (red and purple dots in Figure 8).

Logically, we observe a similar linear increase of 4% of direct damages per year, as well as a similar global increase of around 200% of indirect shocks for both cases. Obviously, indirect damages are always higher when we suppose that all losses are passed onto prices, but what is interesting there is that indirect damages with no pass through are even greater than total damages with pass through. When we have $\phi = 100\%$ for all sectors, indirect damages grow from around 350 billion \$ to 1200 billion \$ on average per year, whereas when the pass-through depends on the sector's price elasticity with the constant c , the indirect damages equal to around 110 billion \$ at the beginning and end at around 370 billion \$.

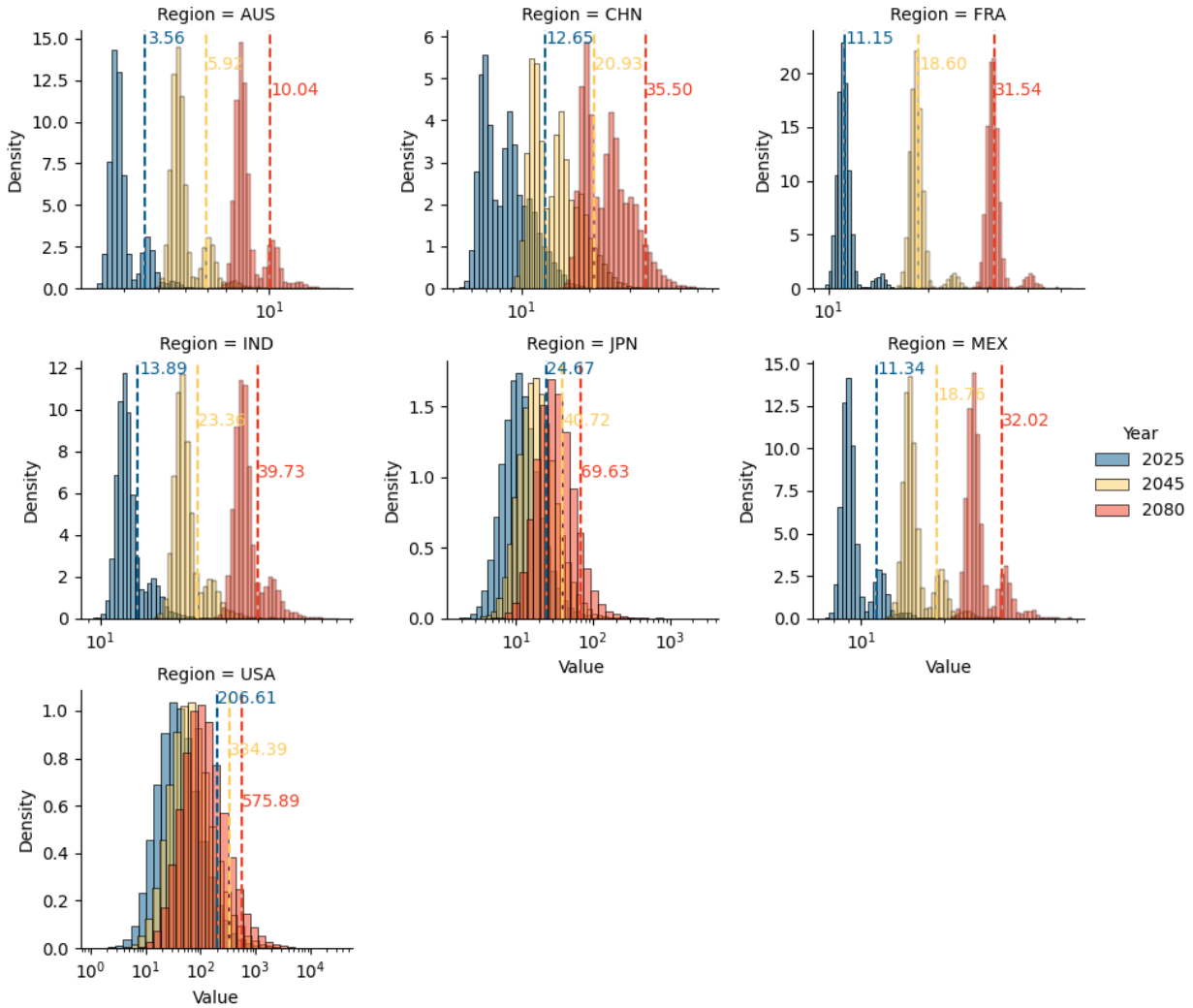
Figure 8: Stochastic ϕ , linear $\mathcal{C}_{SSP-RCP}$ with pass-through using 5,000 iterations


The indirect damages triple the direct losses if there is a 100% pass-through while it is multiplied by about 1.5 if we implement a sector-dependent pass-through. The more sectors and industries are impacted in the world the more sectors are likely to pass their losses onto their prices. In our highly connected economies, such scenario appear very likely.

For instance, in a competitive market, if only one energy industry is affected, it cannot significantly increase its prices as customers may switch to a cheaper alternative. For this reason, we can consider an evolution of the pass-through throughout the years. The number and magnitude of damages caused by extreme events will increase, impacting a higher number of industries in the physical assets dependent sectors. Thus, the losses will be more and more passed onto prices. We can therefore imagine that the pass-through rates will evolve through time to converge to 100%.

Consequently, we can see that direct and indirect damages could amount to about 1.8 trillion \$ yearly damages within the end of the century to be compared to about 300 billion \$ today, still presenting the worst case VaR 95% scenario. If we compute the average yearly direct losses from tropical cyclones since 2000, which amounts to about 85 billion \$, the norm could be 600 billion \$ of losses within the end of the century if no proper action is taken to handle better extreme events, with a rate of return divided by almost 9. Recent examples, Katrina (2005), Harvey, Maria (2017), Hagibis (2019) illustrate the need of important adaptations to address cyclone and more broadly physical risk related extreme events, both at company and government level. We also count 94 storms since 2000 with damages of more than 1% of the gdp of the country since 2000 with countries as big as New Zealand, and we could see this number increase dramatically.

Figure 9: Example of direct shocks distribution - 50 000 iterations with 5 years steps top-down fashion, from 2025 to 2100.



In Figure 9, we have extracted 3 representative years (2025, 2045 and 2080), showing the density of the damages from cyclones of more than 1 billion \$ and more than 1% of gdp and the function and associated calibration introduced in 2.2.3 for chosen countries. The distributions exhibit fat tails with a positive skewness characteristic of the log-normal law, and the frequency of extreme events country by country is visible from each distribution. We can point out the VaR 95% of 207 billion \$ of losses for the USA, which could reach more than half a billion \$ loss within 2080 and the selected assumptions. We can note small peaks of higher values for countries that do not present frequent extreme events (France, Australia, India, and Mexico), matching several events occurring within a same year. The VaR 95 % for the US represents an astonishing 2.2 % shock for the US economy within 2080 with no increase of gdp, given that the trajectories of future cyclones remain relatively equivalent to what they have been in the recent past.

Figure 10: Example of indirect shocks distribution - 50 000 iterations with 5 years steps top-down fashion.

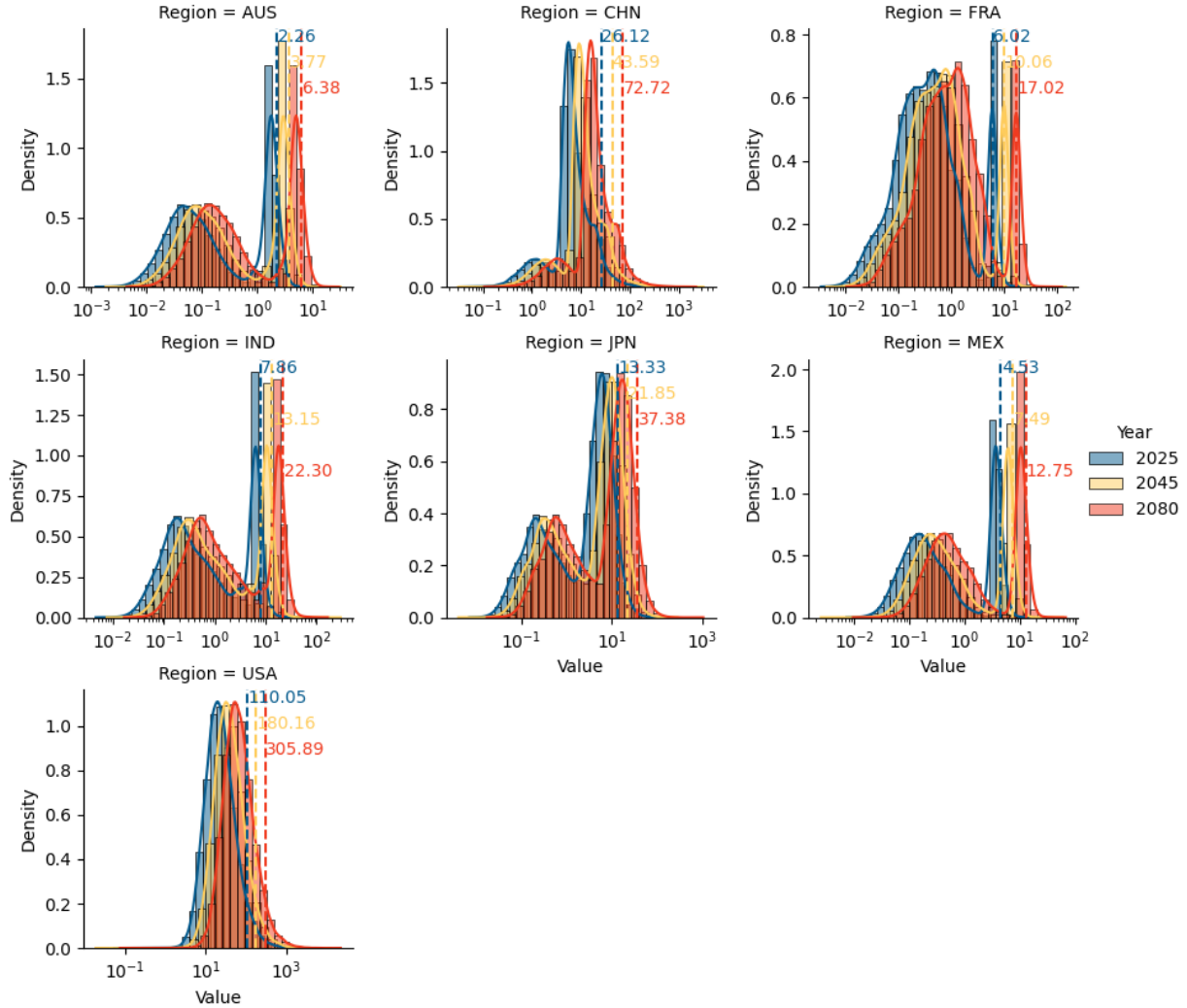
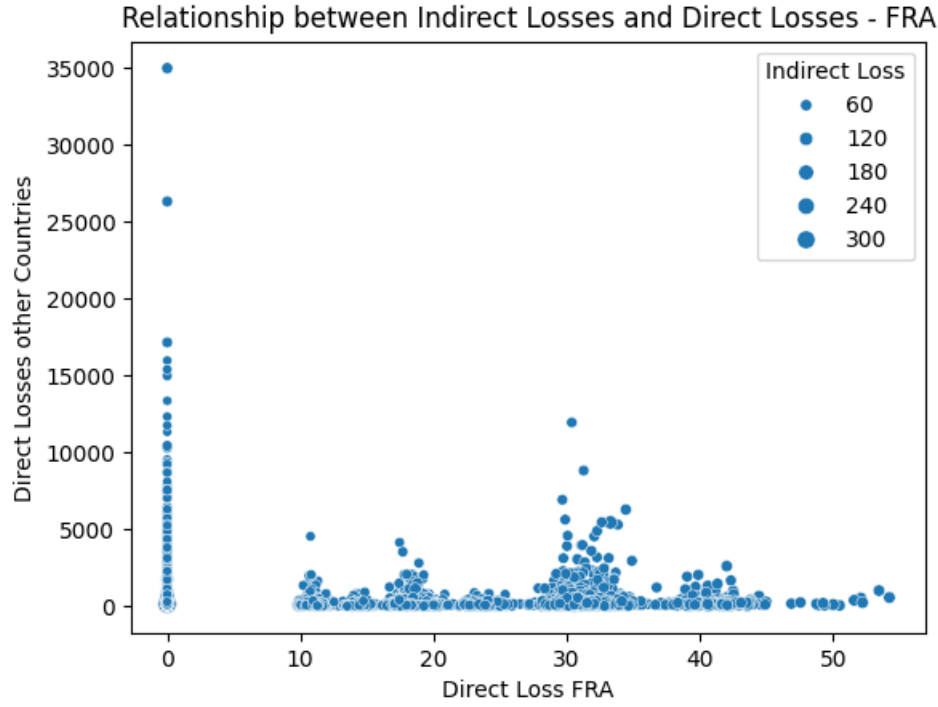


Figure 10 shows the indirect shocks pendant to the direct shocks presented Figure 9. For every country presented here, except the USA, we notice two peaks indicating a bi-modal distribution. For some countries (India, France), the two peaks have about the same height, while for the others, the peak corresponding to higher values is far more pronounced than the other one. The higher part of the bi-modal distribution might be correlated to direct shocks to the country's economy, while the lower part may show correlation to indirect shocks from other economies. The diffusion coefficients are likely to be higher between the sectors of a given country than of extraterritorial origin. For the United States of America, extreme events of large magnitude are frequent, so we would expect less impacts from outside events. We are going to challenge these assumptions in the following figure and analysis.

Statistical testing to identify indirect shocks origin

Relationship between direct shocks and indirect shocks for France.



We notice in this graph that France inherits indirect shocks from direct shocks from other countries (dots matching 0 Direct Loss FRA). Intuitively using this graph, bigger indirect loss values match bigger direct loss values. More than 85% of values are strictly positive, while direct shocks from extreme events (cyclone related) occur globally only 9% of the time.

To confirm and generalize this graphical assumption, we run a significance test at the 99% level using Pearson's correlation coefficient between direct losses from other countries and local direct losses of each country:

$$r_{dl,dlo} = \frac{\sum(x - \mu_x)(y - \mu_y)}{\sqrt{\sum(x - \mu_x)^2 \sum(y - \mu_y)^2}} \quad (51)$$

where $x_{dl,dlo}$ contains direct losses from the country (dl) and from the other countries (dlo) while y contains indirect losses. We obtain r ; Pearson correlation coefficient for each distribution. We then apply a Fisher z-transformation to each coefficient to estimate properly confidence intervals even when the sample correlation coefficient is near -1 or 1:

$$z_{dl,dlo} = \frac{1}{2} \times \ln \frac{1+r}{1-r} \quad (52)$$

Where z is the inverse hyperbolic tangent function.

We then compute the Z-test, suitable for large distributions, the following way:

$$Z_{test} = \frac{z_{dl} - z_{dlo}}{\sqrt{\frac{2}{n-3}}} \quad (53)$$

Here, the Z_{test} statistic equals -495, far below the critical value of -2.33, meaning that the hypothesis that the correlation coefficients between the direct losses of the country, and from other countries, and its indirect losses are similar is rejected with highest confidence. We indeed find a 96% correlation between the direct losses of each country in average and its indirect losses and barely 9% correlation between the direct losses of the other countries and its indirect losses.

Event specific analysis with Hallegatte (2013) Figures 11a to 11c present results from Hallegatte (2013) BoARIO simulations.

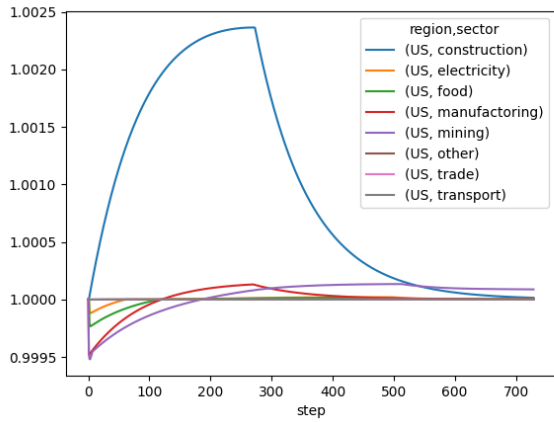
Figure 11a presents the evolution of the realized production of each sector normalized to a starting point of 1. At time 0, a shock of 500 billion USD occurs and impacts a fictive economy. 2 sectors are being affected directly (manufacturing, mining), and 2 sectors are being requested for rebuilding the economy (construction, manufacturing). The shock is proportional to the GDP of the 2 sectors. The most impacted sectors are the ones that suffer direct impacts logically, while construction (with the highest rebuild coefficient of 0.55) is immediately ordered to rebuild and sees its realized production increase to a pick of almost 25 basis points above the starting point. It can cover the rebuilding demand thanks to its capacity to overproduce. The other sectors recover progressively from the shock over the 2-years window of the event.

In Figure 11b we simulate a shock twice as large as the previous one. 5 sectors are being impacted directly (construction, manufacturing, mining, trade and transport), and the same sectors participate to the reconstruction except that, this time, manufacturing contributes up to 60%. Finally, we increase slightly the rebuild factor to 1.1, the rebuild tau to 180 days, and the duration of the event to 8 days. We can observe logically a small plateau with decreased outputs before the economy starts rebuilding itself. Construction that presents a far smaller output than manufacturing is highly boosted by the initial event to around 30 basis points above its starting point.

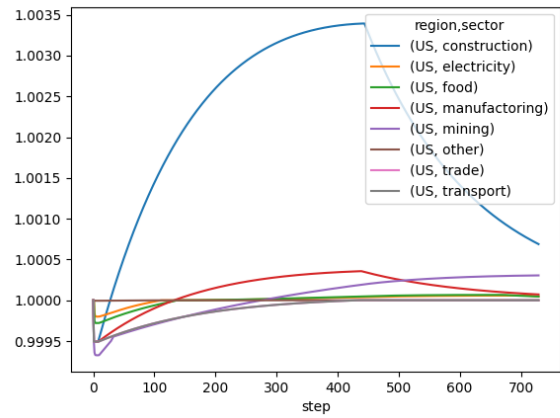
Finally on Figure 11c, we simulate, using BoARIO framework, the impact of a shock matching the 95% VaR of cyclone related direct damages to the US economy. This shock of 207 billion USD is in line with the adjusted damages from Katrina and Harvey that the USA have suffered in recent years. We define affected sectors (NACE) and how each of them has been impacted by the event, and rebuilding sectors and how each of them contributes to the reconstruction of the economy. We also adjust productive capital to value added ratios thanks to figures from the Federal Reserve, the FAO and the European Commission that provides data for economies all around the world. We proxy non available sectors by the global productive capital to value added ratio in the US as of 2022 (3.21). The event lasts 8 days, global rebuild tau is 360 and rebuilding factor is 1. Overproduction capacity is constant and equal to 1.25.

We choose the 12 biggest sectors by gdp (output greater than 2 500 billion \$) and plot the evolution of their realized production for 2 years on a readable graph. We notice that the financial sector suffers the highest impact of about 60 basis points at national level, due to

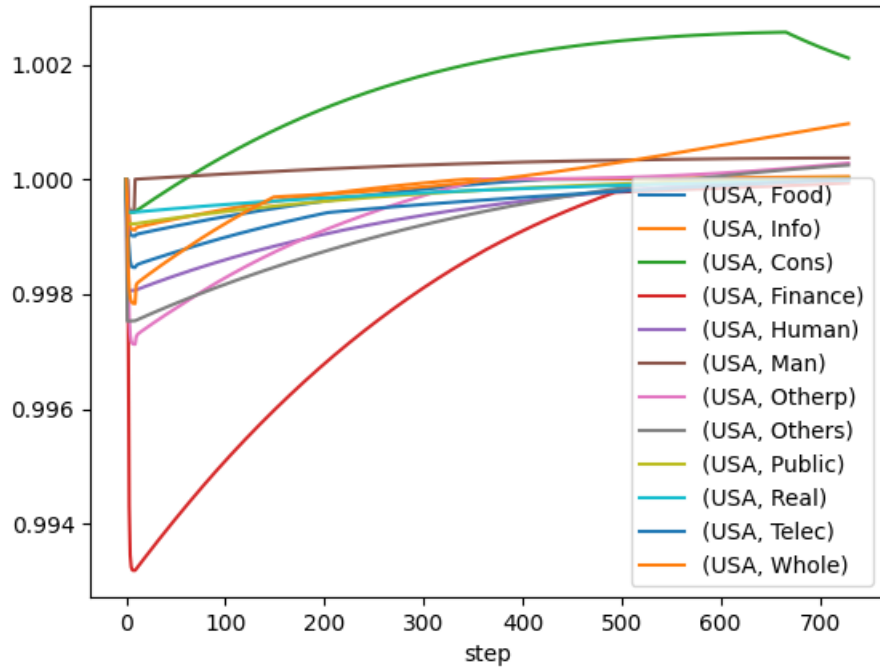
Figure 11: Various simulations using the BoARIO framework



(a) Fictive extreme event



(b) Adjusted endogenous parameters



(c) Realistic event: simulation of a VaR95% level shock on the US economy.^a

^aFood: Accommodation and food service activities. Info: Computer programming, consultancy and related activities, information services. Cons: Construction; Finance: Financial service activities, except insurance and pension funding. Human: Human health and social work activities. Man: Manufacture of food products, beverages and tobacco products. Otherp: Other professional, scientific and technical activities; veterinary activities. Others: Other service activities. Public: Public administration and defense, compulsory social security. Real: Real estate activities. Telec: Telecommunications. Whole: Wholesale trade, except of motor vehicles and motorcycles.

a contagion effect from the insured part of the extreme event. Insurance sector (not shown on the figure for clarity) assumes 40% of the shock with 121 billion \$ of direct and indirect damages. Other sectors in this representation are more resilient with manufacture of food products, beverages and tobacco losing about 5 basis points. Among the sectors affected to rebuilding, construction and wholesale are the ones that benefit the most from this "new activity" (with 21 and 7 basis points respectively), while they also battle for recovery, with wholesale initially losing more than 20 basis points. The recovery of each sector is harder to model and is sector and even firm dependent. Finance should recover pretty quickly while physical assets dependent sectors might take years to recover.

5 Conclusion

The first part of the paper presents a theoretical framework to model physical risk using a bottom-up approach, specifically tailored for use in analyzing physical infrastructure portfolios. ²¹ This method hinges on detailed parameters, including vulnerability curves for each type of extreme event, as outlined in Remark 2.1.1. It is particularly useful for assessing the direct risk exposure of physical assets within portfolios, notably in sectors such as private equity, infrastructure, and businesses heavily dependent on energy or utilities that rely intensively on their physical facilities. Our regional calibration also allows to integrate the important disparities between regions. According to Emdat, Africa and Asia have suffered 221 and 1 022 damage inducing storms since 2000 respectively. But only 9, and 86 of them have provoked extreme losses. In the Americas (mainly in the US), 29% turn out to be extreme events. Less exposed regions today might change in the future with the increase of the population, among other factors.

We have modeled in this paper direct and indirect damages from extreme cyclones worldwide using a 5-years scale from 2025 to 2080, with regional calibration of the damages and a conservative 4% linear annual rise, highlighting 95% VaR. Thus, an extreme event occurring once every 20 years could come back every 4 years within 2050. Our choice of a RCP-SSP with constant GDP aims at improving the readability of our studies. It is also interesting to point out the different distributions of the indirect losses among countries, reflecting specific input/output table structures and direct shocks magnitudes. Finally, with the help of BoARIO framework, we have been able to simulate the rebuilding of the US economy following an extreme event through time, and how every sector behave.

Moreover, our research introduces a technique for disseminating economic shocks caused by disasters at the country level across various sectors and activities. This not only broadens the impact assessment to an international scope but also marks a significant methodological leap. While we base our approach on certain parametric assumptions for the sake of illustration, the framework is designed to be easily adaptable for a more comprehensive application in managing physical risks. Employing a stochastic pass-through rate following beta laws as proposed by Desnos *et al.* (2023), and considering a conservative annual growth rate of 4% of damages specifically calibrated for Tropical Cyclones (TC), we estimate that the average annual economic shocks could surpass 380 billion dollars by 2050, with 70 extreme events per year around the world, 1 every 4 days. Beyond the results of this first experiment, this paper is a methodological contribution to the field of physical risk assessment, proposing an algorithm with relatively low computing cost to estimate the direct and indirect costs of increasing natural disasters on the economies.

It is important to insist on the very parametric and adaptable dimension of this framework. Note that the regional frequency, magnitude, pass-through rates, and increase through time in climate scenarios are all parameters that can be adapted with real time observations. For instance, some countries will face faster increase in flood frequencies than others (countries with low average sea elevation like Bangladesh, Netherlands and China, or countries that face challenges due to excessive drain of groundwater like Mexico or Indonesia), with different responses depending on the capability of answering these challenges (Netherlands

²¹We do not perform the empirical application of this framework in this paper.

have been used to fight flooding for centuries). The population dimension has not been integrated in the simulation, neither for work force modeling and post disaster potential unemployment, or for migration. We could model that a fraction of the population that suffered the extreme event will try to relocate, and thus use this VaR model to simulate the change in migration flux.

With the help of the BoARIO framework, we have been able to go one step further and give deeper sectoral representation, modeling how an economy rebuilds itself following an extreme event occurring once every 20 years in average. Advanced relationships from Hallegatte (2013) related to sectors contributing to the rebuilding of the economy, capacity to overproduce, event duration and precise planning through time are being introduced. To go deeper in the representation, a better share between households and impacted sectors should be the priority. It would also be interesting to consider losses of jobs, interruption of the export industry, tourism industry, oil production and supply, and tax collection as additional financial impacts.

According to CDP's Messenger *et al.* (2023), whenever adaptation plans are in place, they are often costly and present additional risks for publishing companies. According to the World Economic Forum's Global Risk Report for 2023, the failure of climate change adaptation ranks as the second greatest risk for companies over the next 10 years, short only of the failure to mitigate climate change. It also ranks 7 over as short of a period as the next 2 years.

These insights highlight the urgent need for effective adaptation strategies. Given that mitigation efforts are unlikely to substantially change the course of climate change by 2050, it becomes imperative for both corporations and governments to formulate and implement robust adaptation plans to mitigate these risks. This study not only contributes to our understanding of physical risk assessment but also emphasizes the critical need for proactive adaptation in the face of escalating climate threats.

References

- ADENOT, T., BRIERE, M., COUNATHE, P., JOUANNEAU, M., LE BERTHE, T., & LE GUENEDAL, T. (2022). *Cascading Effects of Carbon Price Through the Value Chain: Impact on Firm's Valuation*. Available at SSRN.
- BLACKWELL, C. (2015). *Power Law or Lognormal? Distribution of Normalized Hurricane Damages in the United States, 1900–2005*. *Natural Hazards Review*, 16(3), 04014024. [https://doi.org/10.1061/\(ASCE\)NH.1527-6996.0000162](https://doi.org/10.1061/(ASCE)NH.1527-6996.0000162)
- BLOEMENDAAL, N., de MOEL, H., MARTINEZ, A. B., MUIS, S., HAIGH, I. D., van der WIEL, K., HAARMSMA, R. J., WARD, P. J., ROBERTS, M. J., DULLAART, J. C., et al. (2022). *A globally consistent local-scale assessment of future tropical cyclone risk*. *Science advances*, 8(17), eabm8438.
- CARNEY, M. (2015). *Breaking the Tragedy of the Horizon—climate change and financial stability*. *Speech given at Lloyd's of London*, 29, 220–230.
- DESNOS, B., LE GUENEDAL, T., MORAIS, P., & RONCALLI, T. (2023). *From Climate Stress Testing to Climate Value-at-Risk: A Stochastic Approach*. Available at SSRN 4497124.
- EBERENZ, S., LÜTHI, S., & BRESCH, D. N. (2021). *Regional tropical cyclone impact functions for globally consistent risk assessments*. *Natural Hazards and Earth System Sciences*, 21(1), 393–415.
- EBERENZ, S., STOCKER, D., RÖÖSLI, T., & BRESCH, D. N. (2019). *LitPop: Global Exposure Data for Disaster Risk Assessment*.
- EBERENZ, S., STOCKER, D., RÖÖSLI, T., & BRESCH, D. N. (2020). *Asset exposure data for global physical risk assessment*. *Earth Syst*, 12. <https://doi.org/10.5194/essd-12-817-2020>
- EMANUEL, K. A. (2011). *Global warming effects on US hurricane damage*. *Weather, Climate, and Society*, 3(4), 261–268.
- ESMA. (2022). *Sustainable Finance Roadmap 2022-2024*. European Securities and Markets Authority.
- FERESHTEHNEJAD, E., GIDARIS, I., ROSENHEIM, N., TOMICZEK, T., PADGETT, J. E., COX, D. T., VAN ZANDT, S., & GILLIS PEACOCK, W. (2021). *Probabilistic risk assessment of coupled natural-physical-social systems: Cascading impact of hurricane-induced damages to civil infrastructure in Galveston, Texas*. *Natural Hazards Review*, 22(3), 04021013.
- FINK, J. D., FINK, K. E., & RUSSELL, A. (2010). *When and how do tropical storms affect markets? The case of refined petroleum*. *Energy economics*, 32(6), 1283–1290.
- GUAN, D., WANG, D., HALLEGATTE, S., DAVIS, S. J., HUO, J., LI, S., BAI, Y., LEI, T., XUE, Q., COFFMAN, D., et al. (2020). *Global supply-chain effects of COVID-19 control measures*. *Nature human behaviour*, 4(6), 577–587.
- HALLEGATTE, S. (2008). *An adaptive regional input-output model and its application to the assessment of the economic cost of Katrina*. *Risk Analysis: An International Journal*, 28(3), 779–799.
- HALLEGATTE, S. (2013). *Modeling the role of inventories and heterogeneity in the assessment of the economic costs of natural disasters*. *Risk analysis*, 34(1), 152–167.

- HILSCHER, J., & NOSBUSCH, Y. (2010). *Determinants of sovereign risk: Macroeconomic fundamentals and the pricing of sovereign debt*. *Review of Finance*, 14(2), 235–262.
- HUIZINGA, J., MOEL, H. D., & SZEWCZYK, W. (2017). *Global flood depth-damage functions: Methodology and the database with guidelines*, (KJ-NA-28552-EN-N). <https://doi.org/10.2760/16510>
- KIM, K., & BUI, L. (2019). *Learning from Hurricane Maria: Island ports and supply chain resilience*. *International Journal of Disaster Risk Reduction*, 39, 101244.
- KNAPP, K. R., KRUK, M. C., LEVINSON, D. H., DIAMOND, H. J., & NEUMANN, C. J. (2010). *The international best track archive for climate stewardship (IBTrACS) unifying tropical cyclone data*. *Bulletin of the American Meteorological Society*, 91(3), 363–376.
- KUHLA, K., WILLNER, S. N., OTTO, C., GEIGER, T., & LEVERMANN, A. (2021). *Ripple resonance amplifies economic welfare loss from weather extremes*. *Environmental Research Letters*, 16(11), 114010.
- KUNZE, S. (2021). *Unraveling the effects of tropical cyclones on economic sectors worldwide: Direct and indirect impacts*. *Environmental and Resource Economics*, 78(4), 545–569.
- LE GUENEDAL, T. (2022). *Financial Modeling of Climate-related Risks*. Institut Polytechnique de Paris.
- LE GUENEDAL, T., CHEN, Y.-H. H., PALTSEV, S., DERBEL, Y., LEPETIT, F., MERY, R., SCIAU, A., DUVAL, B., JOUANNEAU, M., KEIP, M., & LE BERTHE, T. (2023). *Climate-Related Stress-Testing and Net-Zero Valuation: A Case Study for Selected Energy-Intensive Companies*.
- LE GUENEDAL, T., DROBINSKI, P., & TANKOV, P. (2022). *Cyclone generation Algorithm including a THERmodynamic module for Integrated National damage Assessment (CATHERINA 1.0) compatible with Coupled Model Intercomparison Project (CMIP) climate data*. *Geoscientific Model Development*, 15(21), 8001–8039.
- LE GUENEDAL, T., & RONCALLI, T. (2022). *Portfolio Construction with Climate Risk Measures*. Available at SSRN 3999971.
- LENZEN, M., MALIK, A., KENWAY, S., DANIELS, P., LAM, K. L., & GESCHKE, A. (2019). *Economic damage and spillovers from a tropical cyclone*. *Natural Hazards and Earth System Sciences*, 19(1), 137–151.
- MANDEL, A., TIGGELOVEN, T., LINCKE, D., KOKS, E., WARD, P., & HINKEL, J. (2021). *Risks on global financial stability induced by climate change: the case of flood risks*. *Climatic Change*, 166(1-2), 4.
- MARVASTI, A., & LAMBERTE, A. (2016). *Commodity price volatility under regulatory changes and disaster*. *Journal of Empirical Finance*, 38, 355–361.
- MEILER, S., CIULLO, A., KROPF, C. M., EMANUEL, K., & BRESCH, D. (2023). *Unraveling unknowns of future tropical cyclone risks*.
- MEILER, S., VOGT, T., BLOEMENDAAL, N., CIULLO, A., LEE, C.-Y., CAMARGO, S. J., EMANUEL, K., & BRESCH, D. N. (2022). *Intercomparison of regional loss estimates from global synthetic tropical cyclone models*. *Nature Communications*, 13(1), 6156.
- MESENTER, S., SIMPSON, P., & KIADEH, R. (2023). *Are companies prepared for the TCFD recommendations?* *cdp.net*.

- PARISIEN, M.-A., KAFKA, V., HIRSCH, K., TODD, J., LAVOIE, S., MACZEK, P., et al. (2005). *Mapping wildfire susceptibility with the BURN-P3 simulation model*.
- SANDBERG, I. W. (1973). *A Nonlinear Input-Output Model of a Multisector Economy*. *Econometrica*, 41(6), 1167–1182.
- SREEPARVATHY, V., & SRINIVAS, V. (2022). *Meteorological flash droughts risk projections based on CMIP6 climate change scenarios*. *npj Climate and Atmospheric Science*, 5(1), 77.
- STADLER, K. (2021). *Pymrio—A Python based multi-regional input-output analysis toolbox*.
- STEENGE, A. E., & BOČKARJOVA, M. (2007). *Thinking about imbalances in post-catastrophe economies: an input–output based proposition*. *Economic Systems Research*, 19(2), 205–223.
- TABARI, H. (2020). *Climate change impact on flood and extreme precipitation increases with water availability*. *Scientific reports*, 10(1), 1–10.
- WEN, J., ZHAO, X.-X., & CHANG, C.-P. (2021). *The impact of extreme events on energy price risk*. *Energy Economics*, 99, 105308.
- WEST, G. R., & JACKSON, R. W. (2004). *Non-Linear Input-Output models: Practicability and Potential*. *Research Papers in Economics*.

A Notation

Table 5: Summary table of the notations

Notation	Description
----- Subscripts -----	
k	company
(i, j)	couple sector-country
i	industry in BoARIO
g	geographic tiles (bottom-up method)
r	region/country
\cdot	variable in question before the disaster
t	time (in years)
----- Variables -----	
S	Direct shock
\mathcal{A}	Total assets of a company k
\mathcal{D}	Damages caused by extreme events
N_g	Number of events (Poisson) in tile g
λ_g	Intensity of Poisson law for event generation
μ_g	Positive drift characteristic of the change of probability of occurrence of extreme event
μ_r, σ_r	Mean and standard deviation for the log-normal law of damages representation
$v_h(r)$	Vulnerability parameter
V	Wind (m.s^{-1})
$f_r, v_n(V, v_h(r))$	Function generating the fraction lost and instrumental variable
θ	Damages modifier for events occurring shortly after another one
ρ	Damages modifier for events impacting different sectors, following a β law
ξ_i	Sectoral shock
$\mathcal{M}_{i,k}$	Market capitalization of sector i and company k
$A, A_{i,j}$	Matrix input-output and its technical coefficients
x_i	Production/supply of the sector i
x^{\max}	Maximum production capacity
y_i	Final demand of the sector i
γ_g^k, Γ_r^k	Density of asset in tile, fraction of revenue in a country
$\gamma_i, \Gamma_{REBUILD}$	Total rebuilding demand, rebuild characteristics time in BoARIO
l_i	Labor input coefficient of the sector i (the amount of labor needed to produce one unit of commodity from sector i)
L	Total labor (employment)
ϕ	Pass-through rate, proportion of the direct losses passed onto prices and other sectors
c	Multiplying constant to convert transition pass-through rate to physical pass-through rate
β	Law for the modeling of the pass-through rate
I	Matrix of imports
$S_D = (c_i)_{1 \leq i \leq n}$	Direct shock matrix or fraction of production lost by the industries after a disaster
t	Total input available after the disaster
E_i	Exportation of sector i
HD_i	Reconstruction demands of households toward the sector i
$D_{i,j}$	Reconstruction demands of each industry i toward each industry j
p_i	Price of the commodity proposed by the sector i / Product built by industry i
Π_i	Profit of sector i
O_i	Amount of orders that industry i is requested to fulfill by other industries
Ω	Inventories/Inputs stock matrix
Γ_{Tot}	Per industry capital lost due to event(s) (destroyed or unavailable)
psi	Inventories heterogeneity parameter
τ_α	Overproduction increase/decrease characteristic time
τ_{INV}	Characteristic time of inventory restoration
$\tau_{REBUILD}$	Characteristic time of rebuilding
α_i^{\max}	Maximum capacity of industry i to overproduce
α_i^b	Base capacity of industry i to overproduce
v_i	Total primary input of sector i / value added ratios
w_i	Exact amount of product p required by industry i to produce x_i
Z	Global transaction matrix in BoARIO
δ_i	Initial or direct shock of production capacity of an industry i

B Complementary materials

 Table 6: Regional vulnerability parameters (in $m \cdot s^{-1}$)

Region	v_{hTDR}^*	v_{hRMSF}^*	\hat{v}_h (chosen)
Caribbean and Mexico	58.8	59.6	59
China Mainland	101.5	80.2	90
USA and Canada	80.5	86	83
North Indian	63.7	58.7	60
South East Asia	60.7	56.7	58
North West Pacific	169.6	135.6	150
Philippines	167.5	84.7	130
Oceania	56.8	49.7	53
South Indian	48.5	46.8	47
Global	98.9	73.4	85

Figure 12: Difference in price sector per sector after the Australian disaster

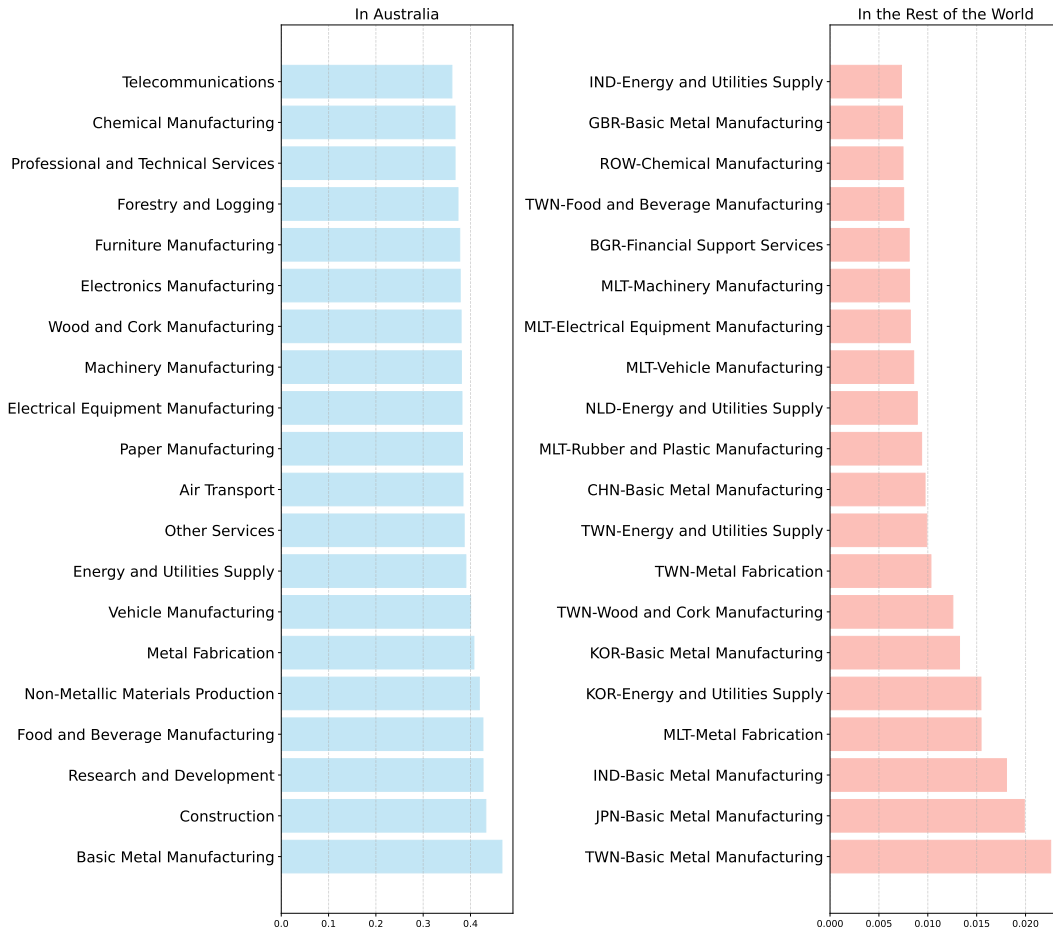


Table 7: Debbie cyclone table of direct shock (Lenzen *et al.*, 2019)

	NSW (Rest)	NSW RT	VIC	QLD B	QLD WBB	QLD DD	QLD SW	QLD F	QLD CW	QLD M	QLD N	QLD FN	QLD NW	SA	WA	TAS	ACT	NT
Sheep	0	0	0	0	0	0	0	0	0	0	0	0	0	0	0	0	0	0
Grains	0	0	0	0	0	0	0	0	0	0	0	0	0	0	0	0	0	0
Beef	0	0	0	0	0	0	0	0	0	0	0	0	0	0	0	0	0	0
Dairy and pigs	0	0	0	0.11	0	0	0	0	0	0	0	0	0	0	0	0	0	0
Other agriculture	0	0.07	0	0	0	0	0	0	0.186	0.53	0	0	0	0	0	0	0	0
Sugar cane	0	0	0	0	0	0	0	0.035	0	0.263	0.112	0	0	0	0	0	0	0
Forestry and fishing	0	0	0	0	0	0	0	0	0	0	0	0	0	0	0	0	0	0
Coal, oil and gas	0	0	0	0	0	0	0	0.056	0	0.053	0.078	0	0	0	0	0	0	0
Non-ferrous metal	0	0	0	0	0	0	0	0	0	0	0	0	0	0	0	0	0	0
Other mining	0	0	0	0	0	0	0	0	0	0	0	0	0	0	0	0	0	0
Food manufacturing	0	0	0	0	0	0	0	0	0	0	0	0	0	0	0	0	0	0
Textiles	0	0	0	0	0	0	0	0	0	0	0	0	0	0	0	0	0	0
Wood and paper	0	0	0	0	0	0	0	0	0	0	0	0	0	0	0	0	0	0
Chemicals, petroleum and coal	0	0	0	0	0	0	0	0	0	0	0	0	0	0	0	0	0	0
Non-metallic mineral	0	0	0	0	0	0	0	0	0	0	0	0	0	0	0	0	0	0
Metals	0	0	0	0	0	0	0	0	0	0	0	0	0	0	0	0	0	0
Machinery appliances and equipment	0	0	0	0	0	0	0	0	0	0	0	0	0	0	0	0	0	0
Other manufacturing	0	0	0	0	0	0	0	0	0	0	0	0	0	0	0	0	0	0
Electricity, gas and water	0	0.004	0	0.001	0	0	0	0.003	0	0.02	0.001	0	0	0	0	0	0	0
Construction (residential)	0	0.016	0	0	0	0	0	0.015	0	0.02	0.013	0	0	0	0	0	0	0
Other construction	0	0	0	0	0	0	0	0	0	0	0	0	0	0	0	0	0	0
Trade	0	0.042	0	0.002	0	0	0	0.017	0	0.013	0.01	0	0	0	0	0	0	0
Accommodation, cafes and restaurants	0	0.22	0	0.005	0	0	0	0.005	0	0.1	0.005	0	0	0	0	0	0	0
Road transport	0	0.016	0	0.002	0	0	0	0.051	0	0.082	0.009	0	0	0	0	0	0	0
Rail and pipeline transport	0	0	0	0	0	0	0	0.014	0	0	0	0	0	0	0	0	0	0
Other transport	0	0	0	0	0	0	0	0.006	0	0	0	0	0	0	0	0	0	0
Communication	0	0	0	0	0	0	0	0.011	0	0.032	0.001	0	0	0	0	0	0	0
Finance, property and business	0	0	0	0	0	0	0	0	0	0	0	0	0	0	0	0	0	0
Ownership of dwellings	0	0	0	0	0	0	0	0	0	0	0	0	0	0	0	0	0	0
Government administration and defense	0	0	0	0	0	0	0	0	0	0	0	0	0	0	0	0	0	0
Education	0	0	0	0	0	0	0	0	0	0	0	0	0	0	0	0	0	0
Health and community	0	0.007	0	0	0	0	0	0	0	0	0	0	0	0	0	0	0	0
Cultural and recreational	0	0.021	0	0.002	0	0	0	0.056	0	0.097	0.006	0	0	0	0	0	0	0
Personal and other services	0	0	0	0	0	0	0	0.055	0	0	0	0	0	0	0	0	0	0

Figure 13: Mean difference prices for the 10 most affected countries after a supposed disaster in Australia calculated via simple diffusion and the WIOD

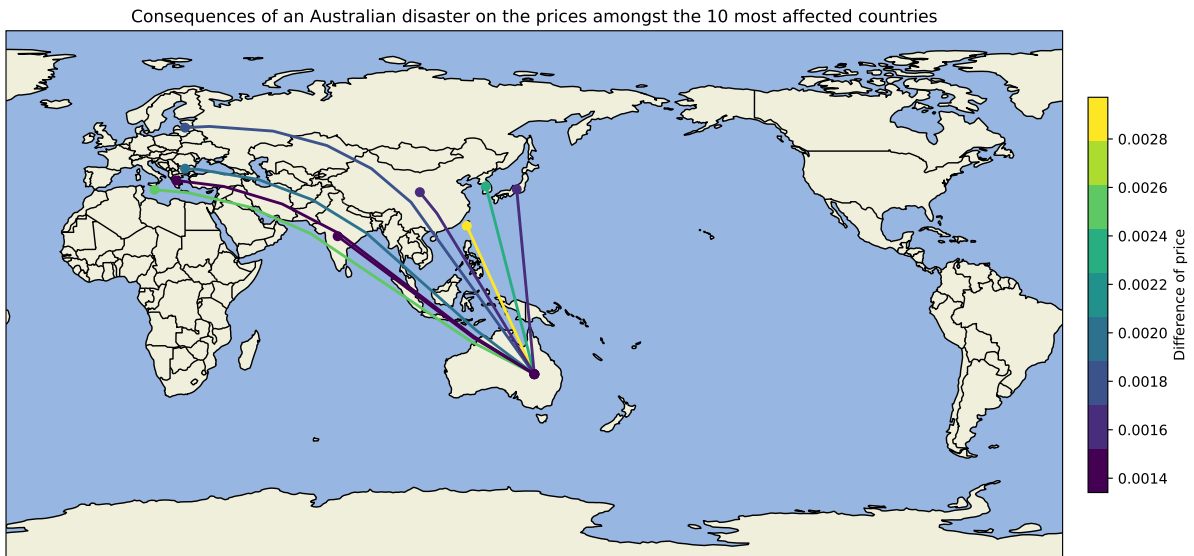


Table 8: Classification of sectors into pass-through types

Type	Sector
highly-elastic	Air transport
	Agriculture
	Chemicals
	Non-metallic minerals
	Paper products
high-elastic	Water transport
	Accommodation and food services
	Pharmaceuticals
	Food and beverages
	Furniture and manufacturing
	Textiles and apparel
	Retail trade
	Financial and insurance services
	Administrative and support services
	Advertising and market research
medium-elastic	Engineering and analysis
	Information services
	Construction
	Financial services
	Forestry and logging
	Legal and accounting services
	Electronics
	Electrical equipment
	Fabricated metal products
	Machinery and equipment
	Transportation equipment
	Rubber and plastic products
	Wood and cork products
	Media production and broadcasting
	Professional and technical services
	Postal and courier services
	Printing and reproduction
	Publishing
	Machinery and equipment repair
	Research and development
Telecommunications	
Warehousing and transportation support	
low-elastic	Water supply
	Wholesale trade
	Extraterritorial organizations
	Household activities
	Education
	Energy supply
	Fishing and aquaculture
	Healthcare and social work
	Insurance and pensions
	Land transport
	Basic metals
	Petroleum products
	Mining and quarrying
Other services	
Public administration and defense	
Real estate	
Waste management	
Motor vehicle trade and repair	

Table 9: Probabilistic characterization of the four pass-through types

		Highly-elastic	High-elastic	Medium-elastic	Low-elastic
Parameters	α	3.0	4.0	14.0	12.0
	β	12.0	6.0	6.0	0.6

Table 10: Number of events damaging either more than 1US\$ Bn or 1% of the country's GDP and their respective total damages in US\$ Bn (adjusted) per region and kind of disaster since 2000

	Count	Total Damage (Mean)	Freq (λ)	95 th Percentile
Drought	63	3.305	2.63	18.536
Africa	4	1.215	0.17	1.684
Americas	20	6.147	0.83	26.474
Asia	22	2.624	0.92	12.800
Europe	13	1.307	0.54	4.173
Oceania	4	1.423	0.17	2.976
Extreme temperature	14	4.546	0.58	24.513
Americas	3	1.949	0.13	2.932
Asia	4	7.964	0.17	27.035
Europe	7	3.705	0.29	16.228
Flood	208	3.808	8.67	37.534
Africa	15	0.793	0.63	4.357
Americas	46	2.478	1.92	16.240
Asia	93	4.908	3.88	47.218
Europe	40	4.512	1.67	32.804
Oceania	14	2.082	0.58	8.754
Storm	376	5.019	15.67	97.794
Africa	9	1.158	0.38	5.461
Americas	228	6.495	9.50	234.079
Asia	86	3.579	3.58	28.628
Europe	27	2.160	1.13	8.605
Oceania	26	1.145	1.08	4.383
Wildfire	29	4.080	1.22	18.563
Americas	21	4.754	0.88	21.471
Asia	1	1.235	0.04	1.235
Europe	5	2.637	0.21	5.126
Oceania	2	2.031	0.08	2.264

Algorithm 2 Illustration of the seminal adaptive approach (Hallegatte, 2008)

y^b the initial final demand vector
 A^b the initial input output matrix
 S fraction shock of the disaster vector
 D additional demand for the industries due to the disaster vector

Inputs α^b initial overproduction capacities
 α^{\max} maximum overproduction capacities
 $\tau_A^\downarrow, \tau_\alpha^\downarrow$ respectively the characteristic times of the decrease of A and α
 $\tau_A^\uparrow, \tau_\alpha^\uparrow$ respectively the characteristic times of the increase of A and α
 I_{local}, J_{local} respectively

$y^t \leftarrow y^b + D$
 $A \leftarrow A^b$
 $\alpha \leftarrow \alpha^b$

for all Δt **do**
 $x^t \leftarrow (I - A)^{-1}y^t$ ▷ first-guess production (Leontiev)
for all industry i **do**
 $x_i^{\max} \leftarrow x_i^t * (1 - S_i) * \alpha_i^t$ ▷ production capacity
 $x_i^t \leftarrow \min\{x_i^t; x_i^{\max}\}$
 $O_i^t \leftarrow \sum_j A_{i,j}x_j^t$ ▷ intermediate consumption
 $x_i^t \leftarrow \min\{x_i^t; \forall j, \frac{x_j^t}{O_j^t}x_i^t\}$
if x_i^t stays unchanged $\forall i$ **then**
STOP
else
 $y_i^t \leftarrow y_i^b + \sum_j A_{i,j}x_j^t$
end if
end for
for all industry j **do**
if $y_j^t > x_j^t$ *id est* if production of industry j not enough to satisfy demand **then**
 $\alpha_j^t \leftarrow \alpha_j^t + (\alpha_j^{\max} - \alpha_j^t) * \frac{y_j^t - x_j^t}{y_j^t} * \frac{\Delta t}{\tau_\alpha^\downarrow}$
for all industry i **do**
if $i \in I_{local}$ and $j \in J_{local}$ or $i \in I_{local}$ and $j \notin J_{local}$ **then**
 $A_{i,j} \leftarrow A_{i,j} - \frac{y_j^t - x_j^t}{y_j^t} * A_{i,j} \frac{\Delta t}{\tau_A^\downarrow}$
else if $i \notin I_{local}$ and $j \in J_{local}$ **then**
 $A_{i,j} \leftarrow A_{i,j} + \frac{y_j^t - x_j^t}{y_j^t} * A_{i,j} \frac{\Delta t}{\tau_A^\downarrow}$
else
 $A_{i,j} \leftarrow A_{i,j}$
end if
end for
else ▷ *id est* when production satisfy demand
 $\alpha_j^t \leftarrow \alpha_j^t + (\alpha_j^b - \alpha_j^t) * \frac{\Delta t}{\tau_\alpha^\uparrow}$
for all industry i **do**

```

if  $i \in I_{local}$  and  $j \in J_{local}$  or  $i \in I_{local}$  and  $j \notin J_{local}$  then
     $A_{i,j} \leftarrow A_{i,j} + \left( \epsilon + \frac{A_{i,j}}{A_{i,j}^b} \right) (A_{i,j}^b - A_{i,j}) \frac{\Delta t}{\tau_A}$ 
else if  $i \notin I_{local}$  and  $j \in J_{local}$  then
     $A_{i,j} \leftarrow A_{i,j} - \left( \epsilon + \frac{A_{i,j}}{A_{i,j}^b} \right) (A_{i,j}^b - A_{i,j}) \frac{\Delta t}{\tau_A}$ 
else
     $A_{i,j} \leftarrow A_{i,j}$ 
end if
end for
end if
end for
end for

```

Figure 14: Diagram of the adaptive methodology (Hallegatte, 2008) for each time t

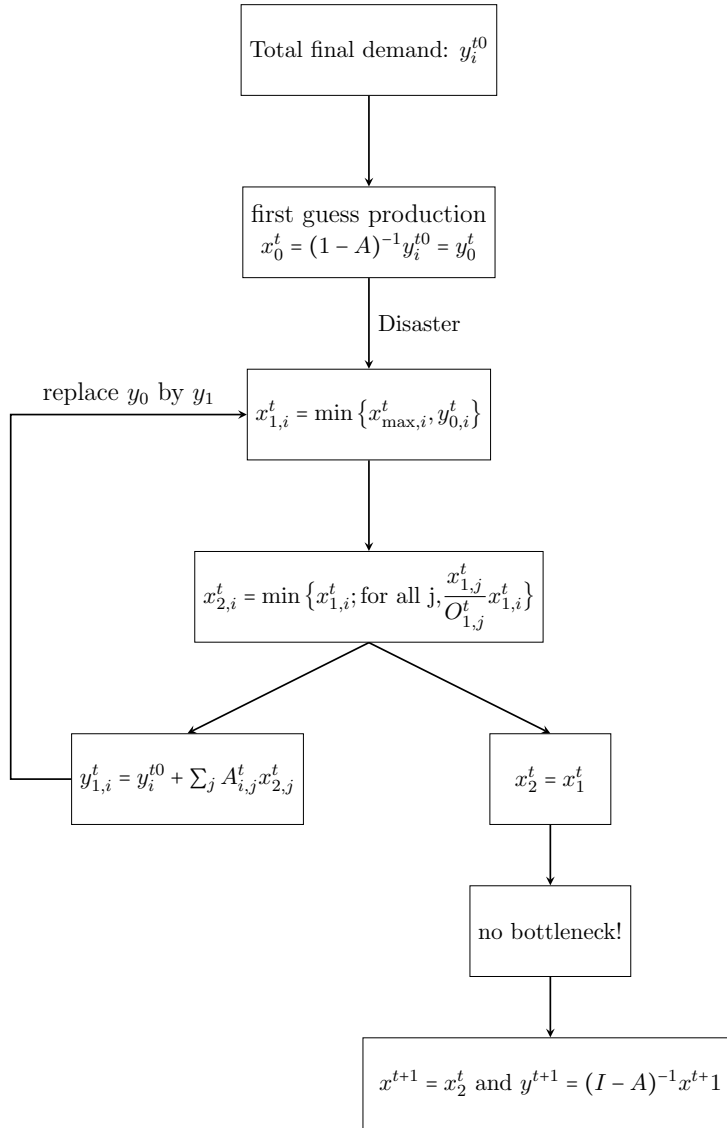


Table 11: BoARIO package events, main inputs and parameters

Parameter	Description
Events	
<i>Recovery</i>	Destroyed capital regained without rebuilding demand and sectors (1)
<i>Rebuild</i>	Destroyed capital is being rebuild through time (2)
<i>Arbitrary production</i>	The production capacity is arbitrarily decreased for a set of industries (3)
Inputs	
<i>t</i>	A time t (in days) to model the evolution of the system following the event (1)(2)(3)
<i>linear, concave, convex</i>	The shape of the recovery function (1)
<i>occurence</i>	Number of events in case multiple events occur simultaneously (1)(2)(3)
<i>duration</i>	In days, before the start of the recovery (1)(2)(3)
<i>rebuild τ</i>	Duration for the rebuilding in days (1)(2)
<i>participation</i>	Proportion of participation of each sector in the reconstruction (2)
<i>rebuilding factor</i>	Lower or greater than 1 rebuilding demand (2)
Parameters	
<i>order type</i>	"alt" if the model uses intermediate order mechanism (no possible substitution) or "classic"
<i>α_{base}</i>	Base overproduction (default 1)
<i>α_{max}</i>	Maximum overproduction (default 1.25)
<i>α_{τ}</i>	Overproduction characteristic time (default 365)
<i>rebuild tau</i>	Rebuilding or recovery characteristic time for events (default 60)
<i>main inv dur</i>	Default initial/goal inventory duration in temporal unit for all sectors if inventory dict is not given (default 90)
<i>infinite inventory sect</i>	List of inputs to never constrain production on
<i>monetary factor</i>	Equal to the monetary factor of the MRIO used (default 10^6 USD)
<i>productive capital to VA dict</i>	A dictionary of sector:ratio format, where the ratio is an estimate of Capital Stock over Value Added ratio (used to estimate the capital stock of each sector)
<i>productive capital vector</i>	Directly sets the capital stock for all industries (overrides Kapital to VA dict)

Table 12: BoARIO VaR95% magnitude event - Affected sectors and weights

Sector	Weight
Activities auxiliary to financial services and insurance activities	5.4%
Air transport	1.3%
Construction	1.7%
Crop and animal production, hunting and related service activities	3.2%
Electricity, gas, steam and air conditioning supply	5.3%
Financial service activities, except insurance and pension funding	1.4%
Human health and social work activities	2.1%
Insurance, reinsurance and pension funding, except compulsory social security	35.4%
Land transport and transport via pipelines	3.9%
Mining and quarrying	15%
Other service activities	3.5%
Public administration and defense, compulsory social security	6.3%
Real estate activities	4.8%
Telecommunications	4.3%
Water collection, treatment and supply	1.1%
Water transport	2.1%
Wholesale and retail trade and repair of motor vehicles and motorcycles	2.1%
Wholesale trade, except of motor vehicles and motorcycles	1.1%

Table 13: BoARIO VaR95% magnitude event - Main rebuilding sectors and weights

Sector	Weight
Construction	25%
Manufacture of machinery and equipment n.e.c.	10%
Manufacture of computer, electronic and optical products	10%
Manufacture of chemicals and chemical products	5%
Manufacture of fabricated metal products, except machinery and equipment	5%
Manufacture of motor vehicles, trailers and semi-trailers	5%
Wholesale and retail trade and repair of motor vehicles and motorcycles	5%



Chief Editor

Monica DEFEND

Head of Amundi Investment Institute

Editors

Marie BRIÈRE

Head of Investors' Intelligence & Academic Partnership

Thierry RONCALLI

Head of Quant Portfolio Strategy

Important Information

This document is solely for informational purposes.

This document does not constitute an offer to sell, a solicitation of an offer to buy, or a recommendation of any security or any other product or service. Any securities, products, or services referenced may not be registered for sale with the relevant authority in your jurisdiction and may not be regulated or supervised by any governmental or similar authority in your jurisdiction.

Any information contained in this document may only be used for your internal use, may not be reproduced or disseminated in any form and may not be used as a basis for or a component of any financial instruments or products or indices.

Furthermore, nothing in this document is intended to provide tax, legal, or investment advice.

Unless otherwise stated, all information contained in this document is from Amundi Asset Management SAS. Diversification does not guarantee a profit or protect against a loss. This document is provided on an "as is" basis and the user of this information assumes the entire risk of any use made of this information. Historical data and analysis should not be taken as an indication or guarantee of any future performance analysis, forecast or prediction. The views expressed regarding market and economic trends are those of the author and not necessarily Amundi Asset Management SAS and are subject to change at any time based on market and other conditions, and there can be no assurance that countries, markets or sectors will perform as expected. These views should not be relied upon as investment advice, a security recommendation, or as an indication of trading for any Amundi product. Investment involves risks, including market, political, liquidity and currency risks.

Furthermore, in no event shall any person involved in the production of this document have any liability for any direct, indirect, special, incidental, punitive, consequential (including, without limitation, lost profits) or any other damages.

Date of first use: 02 May 2024.

Document issued by Amundi Asset Management, "société par actions simplifiée"- SAS with a capital of €1,143,615,555 - Portfolio manager regulated by the AMF under number GP04000036 - Head office: 91-93 boulevard Pasteur - 75015 Paris - France - 437 574 452 RCS Paris - www.amundi.com

Photo credit: iStock by Getty Images - monsitj

Find out more about
Amundi Investment Institute Publications

research-center.amundi.com